



Review

Towards a Highly Efficient ZnO Based Nanogenerator

Mohammad Aiman Mustaffa ¹, Faiz Arith ^{1,*}, Nur Syamimi Noorasid ¹, Mohd Shahril Izuan Mohd Zin ¹, Kok Swee Leong ¹, Fara Ashikin Ali ², Ahmad Nizamuddin Muhammad Mustafa ^{2,3} and Mohd Muzafar Ismail ²

¹ Faculty of Electronic and Computer Engineering, Universiti Teknikal Malaysia Melaka (UTeM), Hang Tuah Jaya, Melaka 76100, Malaysia

² Faculty of Electrical and Electronic Engineering Technology, Universiti Teknikal Malaysia Melaka (UTeM), Hang Tuah Jaya, Melaka 76100, Malaysia

³ Department of Materials, Faculty of Engineering, Imperial College London, London SW7 2AZ, UK

* Correspondence: faiz.arith@utem.edu.my

Abstract: A nanogenerator (NG) is an energy harvester device that converts mechanical energy into electrical energy on a small scale by relying on physical changes. Piezoelectric semiconductor materials play a key role in producing high output power in piezoelectric nanogenerator. Low cost, reliability, deformation, and electrical and thermal properties are the main criteria for an excellent device. Typically, there are several main types of piezoelectric materials, zinc oxide (ZnO) nanorods, barium titanate (BaTiO_3) and lead zirconate titanate (PZT). Among those candidate, ZnO nanorods have shown high performance features due to their unique characteristics, such as having a wide-bandgap semiconductor energy of 3.3 eV and the ability to produce more ordered and uniform structures. In addition, ZnO nanorods have generated considerable output power, mainly due to their elastic nanostructure, mechanical stability and appropriate bandgap. Apart from that, doping the ZnO nanorods and adding doping impurities into the bulk ZnO nanorods are shown to have an influence on device performance. Based on findings, Ni-doped ZnO nanorods are found to have higher output power and surface area compared to other doped. This paper discusses several techniques for the synthesis growth of ZnO nanorods. Findings show that the hydrothermal method is the most commonly used technique due to its low cost and straightforward process. This paper reveals that the growth of ZnO nanorods using the hydrothermal method has achieved a high power density of $9 \mu\text{Wcm}^{-2}$.

Keywords: nanogenerator; zinc oxide (ZnO) nanorods; hydrothermal method; higher output power; piezoelectric effect



Citation: Mustaffa, M.A.; Arith, F.; Noorasid, N.S.; Zin, M.S.I.M.; Leong, K.S.; Ali, F.A.; Mustafa, A.N.M.; Ismail, M.M. Towards a Highly Efficient ZnO Based Nanogenerator. *Micromachines* **2022**, *13*, 2200. <https://doi.org/10.3390/mi1312200>

Academic Editors: Mengying Xie, KC Aw, Junlei Wang, Hailing Fu and Wee Chee Gan

Received: 13 October 2022

Accepted: 1 December 2022

Published: 12 December 2022

Publisher's Note: MDPI stays neutral with regard to jurisdictional claims in published maps and institutional affiliations.



Copyright: © 2022 by the authors. Licensee MDPI, Basel, Switzerland. This article is an open access article distributed under the terms and conditions of the Creative Commons Attribution (CC BY) license (<https://creativecommons.org/licenses/by/4.0/>).

1. Introduction

Urbanization and rapid industrial growth drive the demand for energy resources for human civilization. Since the beginning of the industrial revolution, fossil fuels such as natural gas, petroleum and coal have been the main sources of energy generation. However, the reliance on the use of fossil fuels, which are non-renewable resources, is appalling as they will be depleted in the future. In addition, a lot of pollution and waste from the effects of the use of fossil fuels [1]. Therefore, generating new energy sources as an alternative to traditional fossil fuels is critical and coveted with the increase in the human population. Nuclear, geothermal, tidal, wind and solar energy are viable alternative sources to replace fossil fuels. In general, renewable energy usage mitigates the adverse effects of fossil fuels on the environment, such as environmental contamination and the greenhouse effect [2]. Energy resource constraints can be reduced with the discovery, strategy and generation of these new energy sources but are still not sufficient to meet the demands of social progress [1,3–7]. Therefore, energy generation from portable microelectronic devices is also an alternative to energy generation. These energy sources have the potential to provide humans with a safer, more reliable and stable, and continuous supply of energy [1].

Energy generation technologies have been extensively established with the introduction of miniaturized devices such as electrodynamic, photovoltaic and thermoelectric effects. Some are based on novel concepts, while others leverage advancements in micro-electro-mechanical Systems (MEMS) and nanotechnology, occasionally paired with sensor technology to provide genuinely self-powered sensors [8]. Energy harvesting (EH) is a technique that collects and generates energy from various sources, including mechanical loads, vibrations, temperature and light gradients, generating relatively low force levels in the nW to mW range [9,10]. Mechanical energy harvesting technology has garnered considerable attention due to the pervasiveness of motion and vibration. Research areas include miniaturization, effective batch-production techniques, and wide frequency ranges [8]. Battery replacement is impractical, especially when sensors are placed in inhospitable or difficult locations. Wearable electronics and sensors for on-demand monitoring may result from substantial advancements in low-power electronics. On the other hand, as the Internet of Things (IoT) evolves, it is anticipated that hundreds of millions of low-power sensors will be used globally, reducing or ultimately removing their reliance on battery power via the EH approach [11,12]. Recently, EH such as piezoelectric, electrostatic, electromagnetic, flexoelectric and triboelectric generators are among the technologies that enable mechanical load and vibration conversion [13–19]. Each nanogenerator (NGs) has its own advantages and limitations. For example, a triboelectric nanogenerator (TENGs) can generate high-output voltage but with a relatively small amount of current, due to its high resistance. In general, the internal resistance of a piezoelectric nanogenerator (PENG) is lower than that in TENGs and thus generates much higher voltage and current output, mostly due to its sensitivity. However, for sensing functions, PENGs are more practical and preferred. However, the main disadvantage of these two NGs is degradation and mechanical damage due to external cyclic mechanical stress. The cyclic mechanical stress in TENGs due to the frictional heat generated between the contact layers causes the thermal structure and mechanical properties to change. To overcome that problem, researchers use self-healing materials in NGs. In addition, triboelectricity also suffers from a durability issue, limited short-circuit output current, structural changes and post-stress state [20,21]. On the other hand, pyroelectric nanogenerators (PyNGs) have a high pyroelectric coefficient and low dielectric loss, but it is difficult to achieve a crystalline structure [22].

The piezoelectric effect, which occurs in noncentrosymmetric crystals, is defined as a linear electromechanical interaction between mechanical and electrical conditions; thus, an electric charge accumulates in response to the applied mechanical stress, as shown in Figure 1. The direct piezoelectric effect can be reversed to generate mechanical strain through the application of an electric charge, thus forming an inverted piezoelectric effect [23–27]. Piezoelectric materials, a subset of ferroelectric materials, display a localized charge separation called an electric dipole because of their noncentrosymmetric structure [14,15,17,18,28,29].

Piezoelectric materials are highly desirable for energy-harvesting applications due to the direct conversion of mechanical vibrations to electricity via piezoelectric effects [14,15,18,23–29]. Generally, piezoelectric materials can be classified into two categories, lead-containing (Pb) and lead-free (Pb-free). Lead zirconate titanate ($\text{Pb}_{x}\text{Zr}_{1-x}\text{TiO}_3$, abbreviated PZT) and different modified forms are the most common lead-containing piezoelectric materials, and they have exceptional piezoelectric characteristics. However, due to the harmful effects of Pb elements on humans and the environment, the material's future application is limited. As a result, it is vital to study high-performance materials that are also environmentally friendly (Pb-free). Numerous piezoelectric materials containing no lead have been studied, including barium titanate (BaTiO_3), zinc oxide (ZnO) and polyvinylidene fluoride (PVDF). These materials possess better features in piezoelectricity, structural simplicity, synthesis capabilities, low manufacturing costs and appropriateness for mass production and the application of piezoelectric materials [30–37].

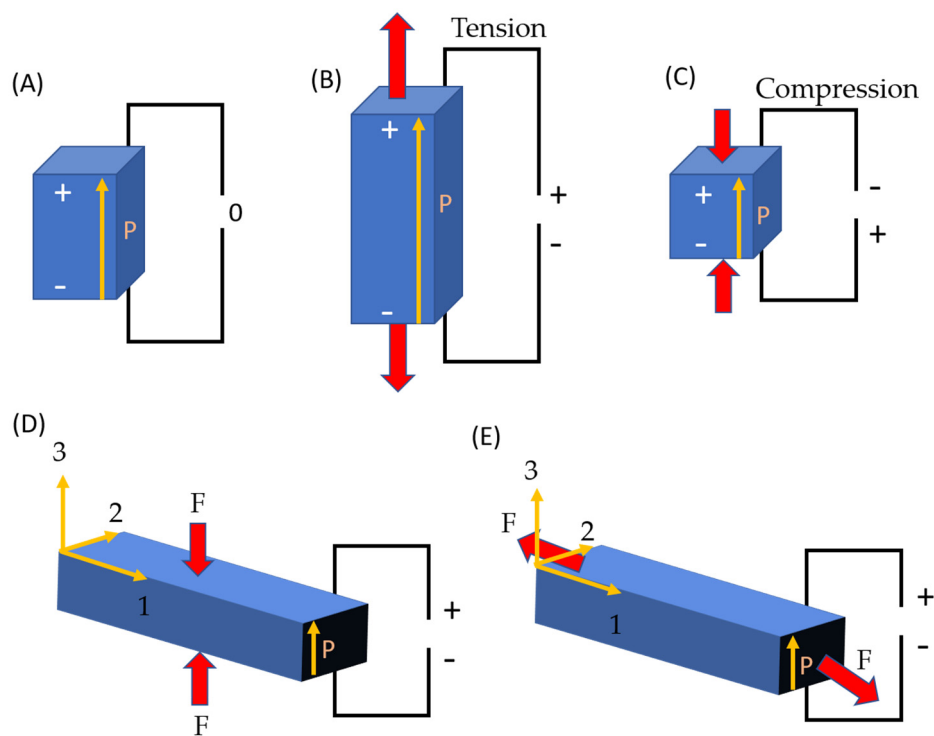


Figure 1. Direct piezoelectric action schematic: (A) electrical charge creation in a piezoelectric material in the absence of an external force, (B) tension and (C) compression. The two most often used operating modes for (D) 33 (stock configuration) and (E) 31 (bending configuration); the pole (producing the net polarization ion) direction is in the order of “3” for both configurations.

2. Piezoelectric Nanogenerator (PENGs)

In 1880, Pierre and Jacques Curie realized the presence of the piezoelectric effect, which occurs in bulk or nanostructured semiconductor crystals, where the central symmetry is broken under the action of an external force, and thus produces the potential for a piezoelectric generation [38]. The PENG is one of the most promising portable energy-harvester devices that was developed by Z. Wang in 2006 [34]. It is a straightforward device that converts mechanical energy to electrical energy through piezoelectric material, and a schematic diagram is shown in Figure 2a [39]. The principle work of PENGs is based on the piezoelectric effect, which means that the electricity is generated under mechanical stress. As a weak force bends a nanowire, piezoelectric potential is generated at its top and bottom. The method of using nanowires (NWs) to generate electricity under the action of external forces represents the power generation function of materials at the nanometer scale. It provides an experimental and theoretical basis for the design of self-powered nanodevices. In 2007, Z. Wang et al. [40] successfully developed a PENG driven by ultrasonic waves to continuously produce output and work in a standalone fashion, as shown in Figure 2b [41]. It consists of a zigzag electrode, a ZnO NWs, a fixed substrate and an external load. This work lays the foundation for the technical transformation and application of nanogenerators, making it a milestone in the field of nanomaterials [41]. Typically, PENGs comprise a piezoelectric layer, a substrate and two electrodes. PENGs use the piezoelectric effect to capture green energy from ocean waves, wind, biomechanical movements and mechanical vibrations in the environment. The output voltage of this type of nanogenerator is influenced by the mechanical deformation and parameters of the piezoelectric layer. Mechanical vibrations in the environment can cause varying deformations in the piezoelectric nanogenerator that generates the AC-output voltage. Nevertheless, a polymeric encapsulation layer technique is proposed to cover the nanostructure layer, providing physical protection, as well as granting chemical and solution stability to the nanodevice [42]. In general, the PENGs have shown appropriate

features due to their structural design, simple performance, simple construction method, high stability and low cost [38].

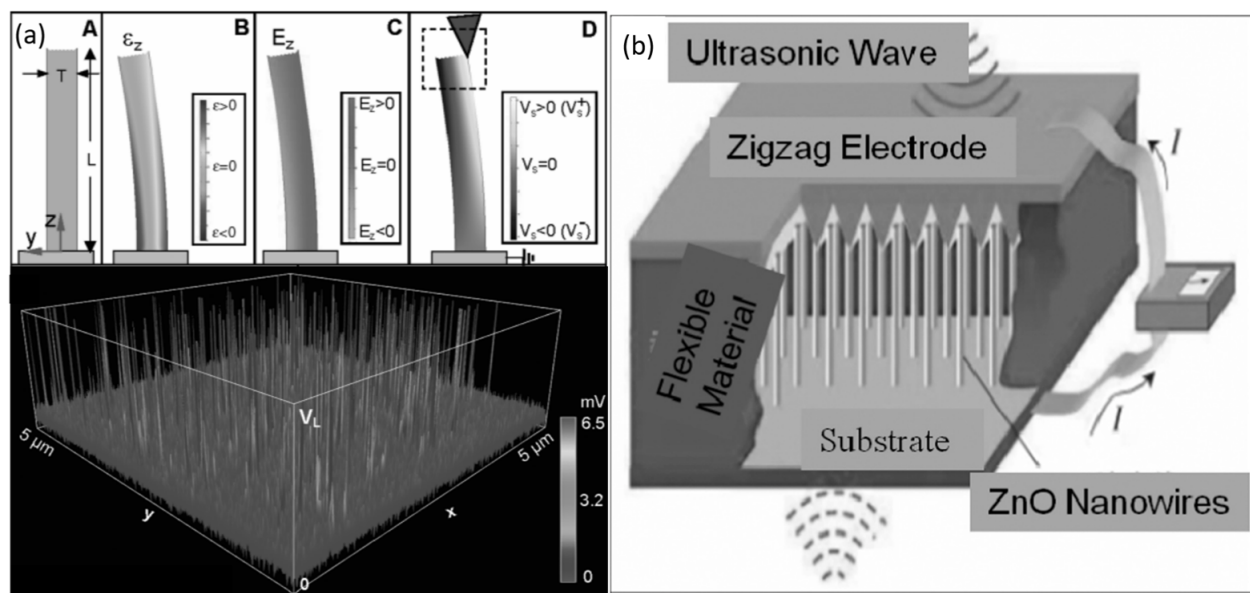


Figure 2. (a) Schematic diagram of (A) PENG nanostructure under (B) longitudinal strain, (C) corresponding longitudinal electric field and (D) potential distribution and (b) the typical structure of PENGs. Reproduced with permission from reference [41].

3. Types of Piezoelectric Material in NGs

3.1. Zinc Oxide (ZnO)

ZnO has been widely used as a piezoelectric nanogenerator due to its excellent structural properties, wherein the lack of a center of symmetry combined with a large electromechanical coupling allows the production of a large piezoelectric response [43]. Kirubaveni Savarimuthu et al. [44] successfully synthesized zinc oxide (ZnO) nanorods (NRs) on a Kapton substrate with a low-temperature hydrothermal method. The ZnO NRs with a silver-electrode-coated insulation layer are purposely to reduce the screening effect and thus increase the output signal strength. Annealing conditions play an important role during the synthesis, wherein the structure of the porous effect can be controlled so as to increase the number of rods that allow a larger contact surface with the counter electrode. This indirectly improves the charge carrier flow mechanism and thus increases the power generated by the device.

Apart from that, Majid S. Al-Ruqeishi et al. [43] fabricated a ZnO NRs-based piezoelectric nanogenerator using an in-tube chemical vapor deposition approach. This technique allows the growth of a high number of ZnO NRs over a large area. It was found that the average length and diameter of ZnO NRs were $3.9\ \mu m$ and $57\ nm$, respectively, as shown in Figure 3, and produced as high as $8.97\ \mu W cm^{-2}$ power density. However, the dimensions of the NRs are non-uniform and rather scattered, resulting in dubious structural quality.

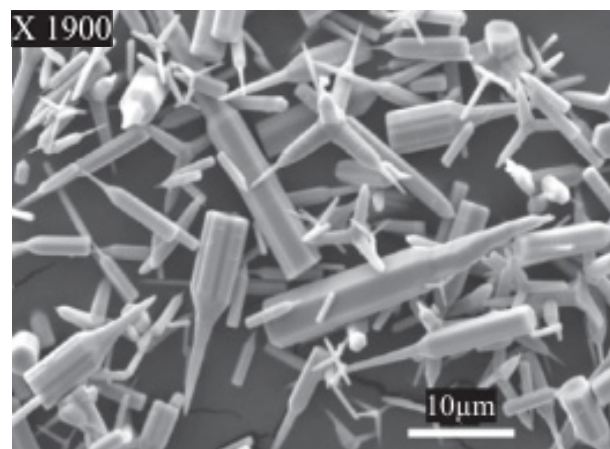


Figure 3. Morphology of ZnO NRs. Reproduced with permission from reference [43].

A polymer coated with a layer of indium tin oxide (ITO) is also widely used as a substrate for ZnO NRs [45]. The polymer substrate offers flexibility in generating energy from the vibration mechanism. In [45], Joe Briscoe et al., synthesis ZnO NRs on /poly(methyl methacrylate) (PMMA) and poly(3,4-ethylenedioxythiophene)poly(styrenesulfonate) (PEDOT:PSS) and found that the internal impedance affects the output power generation, which indicates that the interface state between the substrate and ZnO NRs and the flexibility of the structure cannot be underestimated [45]. However, both ZnO NGs have grown orderly dense ZnO NRs on the polymers, as shown in Figure 4. It is challenging to ensure that ZnO is designed consistently throughout the device manufacturing process, and more ordered structures are required to produce high-performance devices. Compared to other types of ZnO nanostructures, NRs are more promising in the formation of more ordered structures. ZnO NRs can also be produced on various types of substrates with a large surface area. Various deposition techniques have been tried by researchers to create the best arrays of highly oriented ZnO NRs for NG applications [46]. The basic properties of ZnO are shown in Table 1.

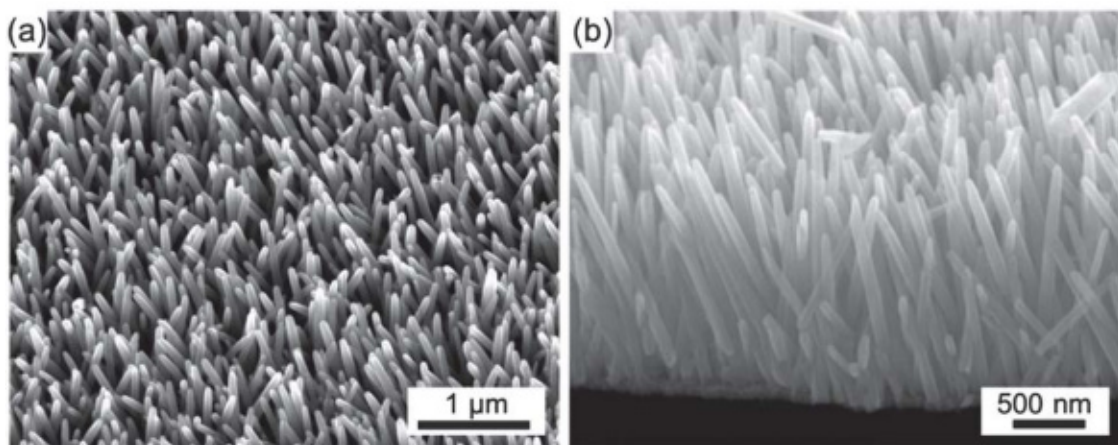


Figure 4. Morphology images of (a) surface and (b) cross-sectional view of the growth of ZnO NRs. Reproduced with permission from reference [45].

Table 1. Fundamental Properties of ZnO [47].

Properties	Value
Lattice parameters at 300 K	
a_0	0.325 nm
c_0	0.521 nm
a_0/c_0	1.602 (ideal hexagonal structure shows 1.633)
u	0.345
Density	5.606 g cm ⁻³
Stable phase at 300 K	Wurtzite
Melting point	1975 °C
Thermal conductivity	0.6, 1–1.2
Linear expansion coefficient (/°C)	$a_0: 6.5 \times 10^{-6}$ $c_0: 3.0 \times 10^{-6}$
Static dielectric constant	8.656
Refractive index	2.008, 2.029
Energy gap	3.4 eV, direct
Intrinsic carrier concentration	<106 cm ⁻³
Exciton binding energy	60 meV
Electron effective mass	0.24
Electron Hall mobility at 300 K for low n-type conductivity	200 cm ² V ⁻¹ s ⁻¹
Hole effective mass	0.59
Hole Hall mobility at 300 K for low p-type conductivity	5–50 cm ² V ⁻¹ s ⁻¹

3.2. Barium Titanate (BaTiO_3)

On the other hands, Aneesh Koka et al. [48] developed a mechanical nanogenerator system utilizing vertically aligned BaTiO_3 nanowire arrays (NWs) as the main semiconducting material. The BaTiO_3 NWs arrays were synthesized on fluoride-doped tin oxide (FTO) glass by a two-step hydrothermal method resulting in a well-structured form, as shown in Figure 5. The aligned nanowire arrays have a higher strain than the bulk layer and thereby improve the power conversion output. It is also found that the vertically aligned BaTiO_3 NGs produce 16 times greater power density compared to the bulk ZnO-based NGs [48]. This shows that the nanorod structure significantly improves the nanogenerator performance, not limited to ZnO materials but also for other semiconductor materials.

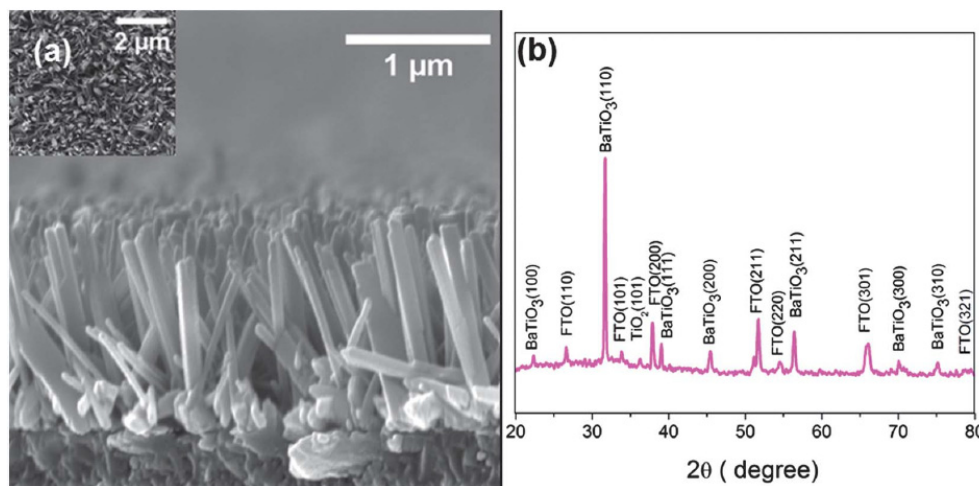


Figure 5. (a) BaTiO_3 NWs arrays in top view. (b) BaTiO_3 constitutes the majority of the peaks in the X-ray diffraction spectra of BaTiO_3 NW arrays. Reproduced with permission from reference [48].

3.3. Lead Zirconate Titanate (PZT)

Ceramics are also used as the main piezoelectric material for NG applications. Weiwei Wu et al. [49] used a robust lead zirconate titanate (PZT) layer on polyethylene terephthalate (PET), which is suitable for flexible and wearable applications, as shown in Figure 6. The developed PZT film is randomly oriented, shrinks and crystallizes after the calcination process, which leads to a fully functional nanogenerator. Compared to ZnO nanowire-

based nanogenerators, the PZT-based device has been shown to exceed the output power density by threefold, indicating the suitability of the PZT-based nanogenerator.

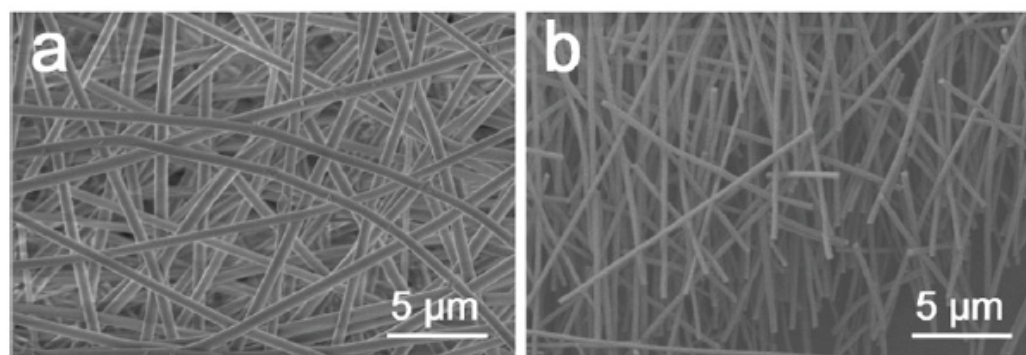


Figure 6. Morphology of PZT NWs (**a,b**). Reproduced with permission from reference [49].

3.4. Indium Nitride (InN)

In 2017, Nai-Jen Ku et al. [50] introduced indium nitride (InN) NWs as the nanogenerator material for a mechanical energy harvester. Obliquely aligned InN NWs have successfully produced adequate output power, exceeding that achieved by ZnO NWs counterparts. However, indium nitride (InN) nanowires are grown on silicon substrates and have not yet been demonstrated on flexible substrates. Recently, first-principles calculations have reported that 2-D InN has high out-of-plane vertical polarization between interlayers in InN, resulting in piezoelectric polarization features. This proves the potential of 2-D InN material to be used as a high-performance nanogenerator [51].

3.5. Other Piezoelectric Materials

In recent years, great efforts have been involved in developing nanoscale energy harvesters or NGs and led to the emergence of many new piezoelectric materials. In 2021, Siju Mishra et al. [52] reported the generation of 2-D zinc sulfide (ZnS) nanosheets for the first time using a simple hydrothermal step. ZnS has high piezoelectric material characteristics, as well as being bio-compatible and non-toxic [53]. In addition, nanocomposite piezoelectric nanogenerator fibers consisting of a combination of poly(vinylidene fluoride) (PVDF) with other materials are also promising [54–57]. A number of PVDF composites have successfully generated large output power and have the potential to be used as nanogenerators, thereby replacing the role of batteries in generating energy. Apart from that, lead-free (K, Na)NbO₃ has also been introduced in energy-harvesting nanodevices [42]. The KNN nanorods were vertically grown in a (100)-orientation on a SrTiO₃ substrate using a hydrothermal technique at low-temperature conditions, which allows the possibility of a ferroelectric nanorods-based device.

Table 2 shows a summary of NGs with different piezoelectric materials, growth conditions, output power and others. Compared to other materials, ZnO NRs generated a large power density as high as $9 \mu\text{Wcm}^{-2}$, as tabulated in Table 2. Based on the findings, ZnO NRs produced high power density with the formation of an organized structure and a large surface area by performing an optimization process. In addition, various deposition techniques have been reported to form highly oriented ZnO NR arrays for PENG applications.

Table 2. A summary of various piezoelectric materials based on nanogenerators.

No	Material	Substrate	Method	Geometry D: Diameter L: Length	Aspect Ratio	Output Voltage [V]	Power Density [Wcm ⁻²]	Ref	Year
1	ZnO NRs	Kapton	Hydrothermal	D: 64 nm L: 1.7 μm	27	400 m	9 μ	[44]	2017
2	ZnO NRs	Quartz tube	Chemical vapor deposition	D: 57 nm, L: 3.9 μm	68	0.74	8.97 μ	[43]	2019
3	BaTiO ₃ NWs	FTO Glass	Hydrothermal	D: 90 nm, L: 1 μm	11	311.5 m	6.27 μ	[48]	2014
4	ZnO NRs/PEDOT:PSS	PET	Thermal evaporation	D: 64 nm, L: 1 μm	16	90 m	5.2 μ	[45]	2013
5	ZnO NRs	Sapphire	Vapor liquid solid	D: 100 nm, L: 1 μm	10	42.5 m	0.4 μ	[34]	2014
6	ZnO NRs/PMMA	PET	Spin coating	D: 64 nm, L: 1.2 μm	19	252 m	0.02 μ	[45]	2013
7	ZnO NRs	Electrospun PVDF fibers	Hydrothermal	D: 30 nm, L: 183 nm	6	79.95 m	0.91 n	[58]	2018
8	ZnO NRs	Terylene-fabric	Hydrothermal	D: 200 nm, L: 5 μm	25	10 m		[59]	2014
9	BaTiO ₃ nanotube	Titanium	Hydrothermal	D: 144 nm, L: 6 μm	42	6.3 m		[60]	2020
10	ZnO NRs	Cotton Fabric	Aqueous chemical growth	D: 200 nm		9.5 m		[61]	2012
11	PZT nanofibers	Silicon	Electrospinnig process	D: 100 nm, L: 85 μm		0.4 m		[62]	2009
12	Indium nitride nanowire	Silicon		D: 43 nm		825 μ	2.9 n	[50]	2017
13	Indium nitride					0.195	73 m	[51]	2021
14	Zinc sulfide nanosheets	flexible aluminum	Hydrothermal			600 m	219.5 n	[52]	2021
15	Zinc sulfide nanofibers		Hydrothermal	D: 600 nm		3		[53]	2020

4. Effect of Dopant on ZnO Nanorods (NRs) Piezoelectric Nanogenerator (PENGs)

The ZnO PENGs, PZT and BaTiO₃ have distinct characteristics. The performance of PENGs can be enhanced by altering the micromorphology of the piezoelectric material. However, the improvement is very marginal. Researchers have introduced chemical techniques to increase the piezoelectric coefficients in piezoelectric materials, thereby improving the piezoelectric properties of the material and the performance of the piezoelectric nanogenerators [41,63]. The piezoelectric coefficients and dielectric constants of the piezoelectric material can be altered by the addition of a small amount of doping into the piezoelectric main material, resulting in a more productive energy generation process. For instance, ZnO, which is a high-performance semiconductor material, can be adapted with two distinct doping strategies: N-type doping and P-type doping. Doping with n-type elements provides an increase in the crystalline lattice tension along the ZnO crystal axis and increases the piezoelectric coefficient, thus improving the output performance of the PENGs. However, these dopant ions have the feature of being overly permeable and produce excessively high doping concentrations. As a result, more lattice defects can arise in this circumstance, obstructing charging on external circuits and reducing energy generation performance. The effects of free electron protection caused by doping in ZnO can be minimized by the use of the p-type dopant [41].

4.1. Silver-Doped (Ag-Doped) ZnO Nanorods (NRs)

Sumera Rafique et al. [64] developed a PENG based on Ag-doped ZnO NRs on cotton fabrics, as shown in Figure 7. In general, the potential is generated due to the piezoelectric action originated from the relative dislocation of Zn^{+2} cations and O^{-2} anions in the wurtzite crystal structure. Both undoped and Ag-doped ZnO nanorods-based nanogenerators exhibit good arrangement synchronization, implying that the maximum number of NRs generates piezoelectric potential simultaneously and in the same direction. However, it was found that the Ag-doped device produced three times the power generation compared to the undoped ZnO NRs-based PENGs [64]. This is possibly due to the reduction of free charge concentration by the Ag-doped passivation. The grown Ag-doped ZnO NRs are dense, oriented and have formed an appropriate atomic diameter of Ag-doped ZnO NRs, as shown in Figure 8, which allow the formation of excellent interfaces with the hydroxyl groups of cotton fabrics.

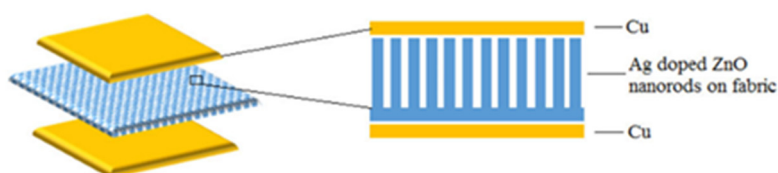


Figure 7. Schematic diagram of a piezoelectric nanogenerator based on Ag-doped ZnO NRs. Reproduced with permission from reference [64].

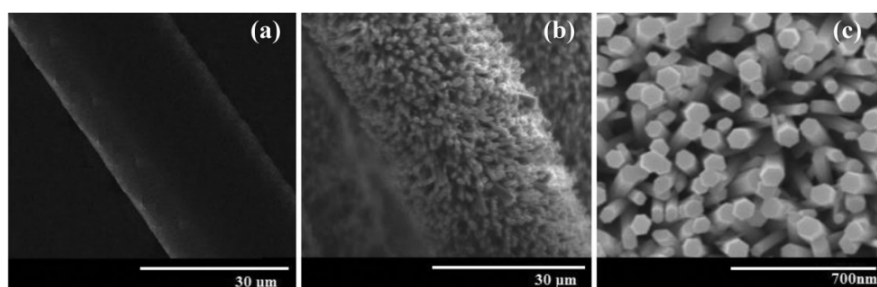


Figure 8. (a) Observation of a cotton fiber without ZnO development, (b) picture demonstrating the presence of Ag-doped ZnO NRs on a cotton fiber, (c) better magnification image of Ag-doped ZnO NRs on a cotton fiber. Reproduced with permission from reference [64].

Furthermore, Ag doping assists in reducing the growth of nucleation activation energy in ZnO NRs and also results in an increase in the NR diameter [64]. The addition of the Ag dopant also keeps the growth process at a lower temperature, allowing the fabrication of devices on flexible substrates.

4.2. Aluminium Doped (Al-Doped) ZnO Nanorods (NRs)

Wen Yang Chang et al. [65] developed a PENG based on Al-doped ZnO (AZO) nanorods with a V-zigzag layer, as depicted in Figure 9. The AZO layer is grown at a low temperature on ITO glass, using an aqueous solution approach. The V-zigzag structure improves the bending and compression deformation characteristics of the NGs. Interestingly, the AZO NGs successfully generate output power at an ultra-low temperature, near to liquid helium state. This proves that the AZO NGs are reliable and can be used as an energy harvester even under extreme conditions.

In addition, the concentration of the Al dopant in ZnO NRs also affects device performance [66]. Aqueous solutions provide an excellent medium for the process of dopant concentration optimization. This process is promising and has attracted much attention due to being able to produce controlled, highly compact and highly oriented ZnO nanostructures [66,67].

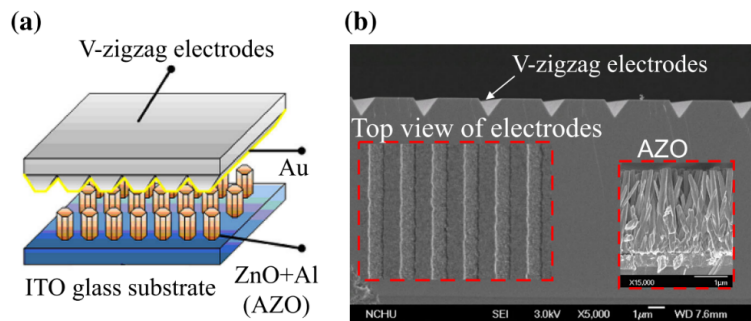


Figure 9. Mechanism energy harvesting based on V-zigzag electrodes: (a) AZO and V-zigzag structure, (b) SEM pictures of AZO NRs. Reproduced with permission from reference [65].

4.3. Nickel Doped (Ni-Doped) ZnO Nanorods (NRs)

Nickel (Ni) has been widely used in semiconductor materials as a dopant for various applications in improving charge transfer performance and also in passivating defects in the host materials. There are many similarities between the valence of Zn^{2+} and Ni^{2+} , allowing the vacancy defects of Zn^{2+} to be easily passivated by Ni^{2+} . This is also due to the ionic radii for Zn^{2+} and Ni^{2+} being almost similar, 0.074 nm and 0.069 nm, respectively, allowing the transport and separation of charges to be enhanced [68]. In 2020, Yen-Lin Chu et al. [68] introduced the Ni-doped ZnO NRs NGs that were grown by chemical bath deposition on the ITO substrate. Compared to the pure ZnO NRs NGs, the Ni-doped device shows a dense nanorod structure as shown in Figure 10. In addition, the output power is also enhanced by three-fold than that obtained for the pure ZnO NRs NGs. Ni-doped ZnO has also been used as a nanocomposite filler and has improved the piezoelectric characteristics of NGs [69].

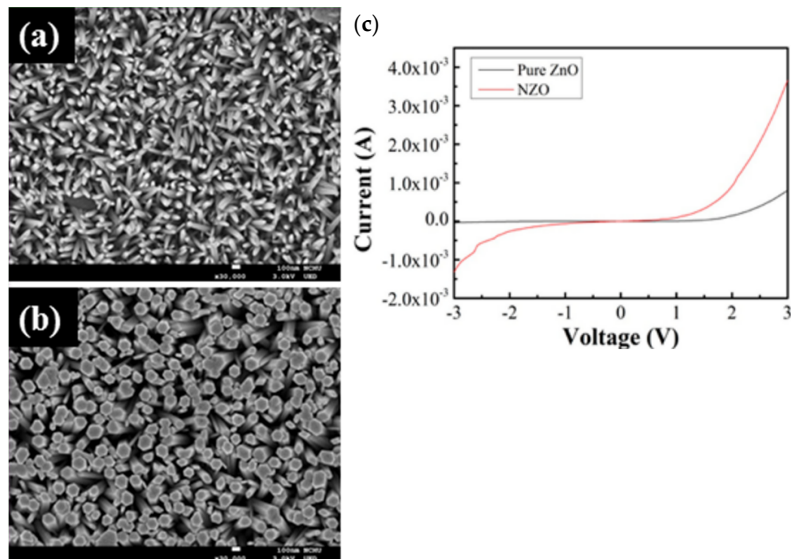


Figure 10. Shows the top view of pure ZnO NRs and Ni-doped ZnO NRs structure (a,b) using FESEM and the IV characteristic of Pure ZnO and Ni-doped ZnO NRs (c). Reproduced with permission from reference [68].

4.4. Rare Earth Material ZnO Nanorods (NRs)

The rare-earth-doped ZnO NRs NGs significantly improved the piezoelectric properties and response. Recently, several researchers adopted the idea and reported promising results. Nd-doped [70], La-doped [71], Tb-doped [72] and Ce-doped [73] ZnO nanorod nanogenerators have shown very encouraging findings. It was documented that the rare-earth-doped ZnO nanorod nanogenerator devices increased the output power by at least three times

compared to pure ZnO NRs. This clearly shows the upright effect obtained by adding rare earth ions into the ZnO NRs in increasing the performance of generated energy.

4.5. Other Dopants in ZnO Nanorods (NRs)

Researchers also devoted a great deal of effort in other dopant material in ZnO NR NGs to improve the output power generation. The chemical modification of the ZnO NRs has proven to be a successful strategy to increase energy-harvester performance. Various research groups have reported vanadium (V⁵⁺)- [74], barium (Ba)- [75], gallium (Ga)- [76], Cr- [77], and S [78]-doped ZnO NRs NGs. Overall, the results show a positive effect provided by all dopants. Modifications to the bandgap, ZnO matrix and passivation defects are believed to occur with the presence of the dopant. Among the dopants, Ni and La elements have shown remarkable power density output compared to others when incorporated with ZnO material as nanogenerator. This is most probably due to the appropriate ionic radii diameter with Zn²⁺. It is well known that the Zn²⁺ vacancies are the main site defects that contribute the charge carrier deficiency and thus degrade the device performance. Thus, incorporating dopants with almost similar ionic radii diameters will effectively replace or passivate the Zn²⁺ vacancies, thereby increasing the power density generation.

Table 3 shows the summary of all dopants in ZnO NRs NGs. Based on the findings, Ni-doping is promising and has achieved high output power up to 735 mWcm⁻². This is possibly due to the highly magnetic behavior of nickel [79] and also the higher surface area covered by Ni-doping over the ZnO nanorods layer [80].

Table 3. A summary of various dopants in ZnO nanogenerators.

No	Material	Substrate	Method	Geometry D: Diameter L: Length	Aspect Ratio	Output Voltage [V]	Power Density [Wcm ⁻²]	Ref	Year
1	Ni-Doped ZnO NRs	Glass	Chemical bath deposition	L: 1.72 μm		0.07	735 m	[68]	2020
2	Ag-doped ZnO NRs	cotton fabric	Hydrothermal	D: 86 nm		6.85	1.45 m	[64]	2019
3	Al-doped ZnO NRs	Glass	Chemical aqueous solution	L: 1.81 μm		1.35 m	1.026 n	[65]	2015
4	Al-doped ZnO NRs	Glass	Chemical solution	D: 70 nm, L: 1.75 μm	25	60 m	0.84 n	[81]	2010
5	Ag-doped ZnO NRs	PET	Hydrothermal	D: 110 nm, L: 2.02 μm	18	5.2 m		[82]	2017
6	PVDF-HFP/Ni-doped ZnO nanocomposites		Hydrothermal			1.2		[69]	2017
7	Neodymium (Nd)-doped ZnO NRs	PET	Wet chemical coprecipitation	D: 101 nm L: 412 nm	4	31		[70]	2018
8	La-doped ZnO		Wet chemical	D: 60 nm		1.6	50 m	[71]	2019
9	Tb-doped ZnO nanotapers		Wet chemical coprecipitation			2.3		[72]	2020
10	Ce-doped ZnO nanoparticles		Wet chemical solution	D: 18 nm L: 100 nm	6	2.5		[73]	2014
11	Vanadium-doped ZnO nanosheet	PET	Cost-effective seed-assisted solution	D: 100 nm L: 1.5 μm	15			[74]	2013
12	Ba-doped ZnO NRs		Wet chemical coprecipitation	D: 73.25 nm L: 476.51 nm	7	10.5		[75]	2021
13	Ga-doped ZnO NRs	PES	An aqueous solution	D: 75 nm				[76]	2012
14	Cr-doped ZnO NRs		Wet chemical solution	D: 300 nm		8 m		[77]	2014
15	S-doped ZnO NRs		Hydrothermal	L: 2 μm		150 m	24 n	[78]	2022

5. Synthesis Techniques of Growth Process ZnO

Over few past decades, ZnO NRs have attracted a lot of attention among researchers for energy-harvester materials, owing to its excellent physical properties [83]. Properties, such as piezoelectric features, high thermal conductivity, high catalytic capabilities, UV filtering capability, semiconductor and antifungal and antibacterial effects have marked ZnO as a well-established material in the electronic, cosmetic and medical fields alike [84]. The synthesis of ZnO nanostructures can be approached by a variety of different methods, resulting in a wide range of different nano-structures. The piezoelectric properties of ZnO NRs are greatly influenced by the synthesis technique used in growing ZnO NRs. The surface morphology of ZnO NRs [85,86], structure orientation [87], crystallinity [88], and majority charge carriers of ZnO nanorods [89,90] can be highly tuned by choosing an accurate synthesis method. In this section, the synthesis methods that have formed the finest ZnO NRs for PENGs applications are discussed, among which are chemical vapor deposition (CVD) and hydrothermal and electrochemical deposition.

5.1. Chemical Vapor Deposition (CVD) Technique

Chemical vapor deposition is a common technique to grow ZnO NRs for large-scale production. ZnO NRs are grown using zinc powder and zinc oxide powder precursors in a horizontal tube furnace, as illustrated in Figure 11. Typically, the synthesis temperature is in a range between 450 °C to 900 °C for zinc powder [91,92], while 1200 °C and above for zinc oxide powder [93]. Both precursors release zinc vapor phase, which is then adsorbed on the surface of the heated substrate and simultaneously reacts with oxygen for the growth of ZnO NRs. Factors that affect the morphology and piezoelectric characteristics of ZnO NRs developed with this technique include the type of substrate used [94], [95], vacuum pressure [96], type of carrier gas [97], and synthesis temperature [98]. In this way, ZnO nanorods are grown vertically with a uniform geometry, thus allowing more electrical contact with the electrode. Vertically aligned ZnO NRs are well grown on substrates with minimal lattice mismatch with ZnO, such as α -Al₂O₃, TiN epilayer, GaN/Al₂O₃, graphene/Al₂O₃ and 4H-SiC epilayer. Typically, ZnO NRs produce high crystal quality by using the CVD technique due to relatively high synthesis temperatures [98]. However, the CVD method is a vacuum-based technique that incurs high operating costs and also requires a high synthesis temperature reaching over 450 °C, which is not suitable for polymer substrates.

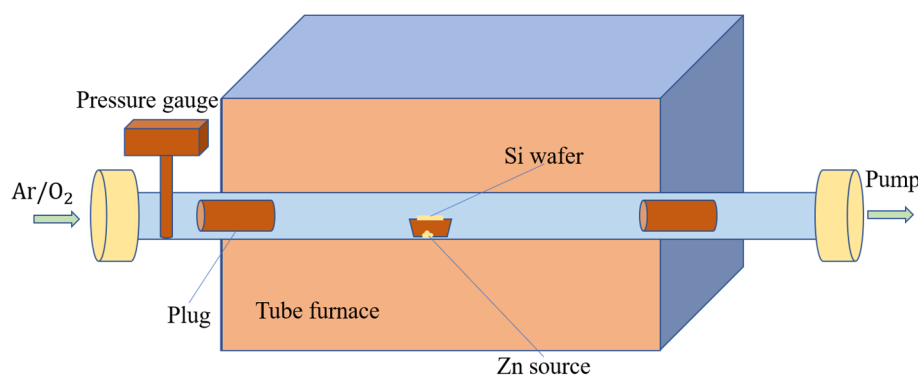


Figure 11. Schematic diagram of CVD process for ZnO NR growth in a horizontal tube furnace.

5.2. Hydrothermal Technique

Recently, researchers have focused on synthesis techniques via a wet chemical path in forming the ZnO NRs. Generally, the ZnO NRs can be grown on a flexible polymer substrate, which requires a relatively low synthesis temperature, i.e., below 100 °C. The hydrothermal technique is the most widely used for ZnO NRs synthesis method and has demonstrated a highly oriented ZnO NRs [99]. A large number of ZnO NRs have been successfully grown on flexible substrates for NG application such as polyethylene

terephthalate (PET) [100], polycarbonate (PC) [101–103], carbon fiber [104], poly(methyl methacrylate) (PMMA) [105], textile fabric [106–108], Ti foil [109], graphene-coated polyethylene terephthalate [110] and polyethylene naphthalate (PEN) [111]. There are two steps involved in this synthesisL seeding on the substrate, followed by the growth of ZnO NRs on the seed layer, as shown in Figure 12. A seed layer of ZnO is pre-deposited on the substrate in order to facilitate the growth process of ZnO NRs on the substrate. In addition, the ZnO seed layer is one of the factors that significantly affect the morphology of ZnO NRs. Therefore, it is one of the crucial factors that must be considered in order to produce the best ZnO NRs. There are several methods that can be used to deposit the ZnO seed layer, such as radio frequency (RF) sputtering [63,101,112–115], spin coating [116], electro-spraying [117] and the atomic layer deposition method [118]. After the seed layer is deposited, the substrate is placed in an autoclave filled with a zinc precursor solution. The pH of the zinc precursor solution can be adjusted with sodium hydroxide and/or hydrochloric acid, since the optimal pH for the growth of ZnO NRs on seeded substrates is between 7 and 10 [119,120]. Thus, for the ZnO NRs growth process, the ZnO NRs synthesis process is started first by dissolving zinc nitrate hexahydrate into distilled water. Generally, the growth temperature of ZnO by using hydrothermal method is between 85 to 100 °C, which is suitable for polymer substrates, and the duration of the growth process of ZnO NRs varied from 3 to 12 h.

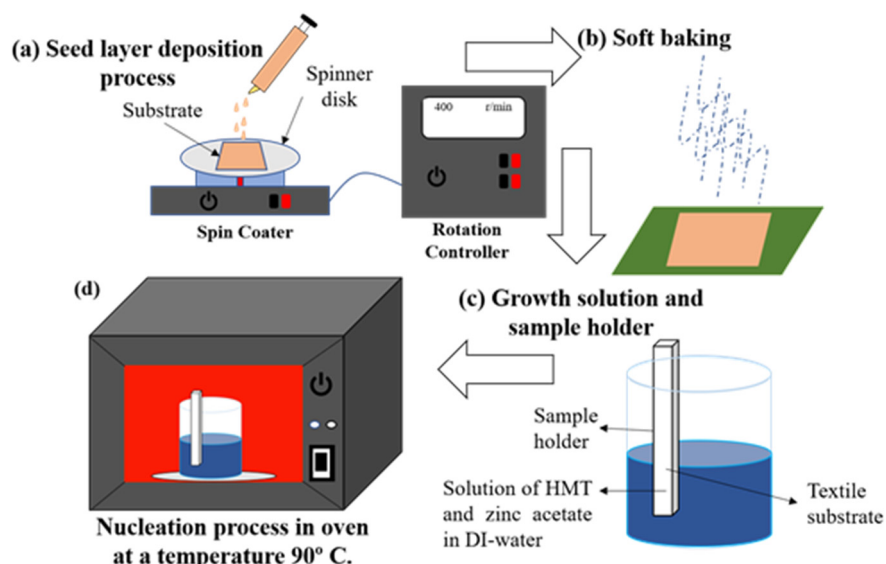


Figure 12. Schematic diagram of hydrothermal process for ZnO NRs.

Tao et al. [121] found that seed layers prepared under different oxygen partial pressure sputtering parameters and annealing treatments had a great influence on the morphology of ZnO NR arrays. It also stated that the average length and diameter of ZnO NRs grew as the pH solution increased, and the optimal pH range for well-aligned ZnO NRs growth was between 10 to 10.4 for a 40 nm-thick zinc seed layer [122]. In conclusion, the alignment of ZnO NR synthesis through the hydrothermal technique is highly reliant on the preferred crystal orientation of the ZnO seed layer. The hydrothermal technique has attracted the attention of many researchers due to its numerous advantages. It is a simple procedure that generates little heat and yields high results at a low cost. Furthermore, it is a fast and controlled technique that can produce structures that are good in terms of shape and clarity [123].

5.3. Electrochemical Deposition Technique (ECD)

Electrochemical deposition (ECD) is a surface modification process in which a thin and strongly adherent coating of metal, oxide, salt or macromolecules is deposited onto a conducting substrate by the simple electrolysis of a solution containing the desired sub-

stance. Besides ECD, this technique is also known as electro-deposition, electroplating or electrolytic deposition [124]. ECD has several advantages over other deposition techniques, including its simplicity, low cost, low temperature, high deposition rate and suitability for substrates with a large surface area. This method is therefore one of the most effective methods for growing ZnO thin films. A thin layer of ZnO can be made on any conductive substrate, including transparent conducting oxide or any other metal plate through this ECD technique, wherein merely low cathode voltage or current is required [125]. In addition, ECD is similar to hydrothermal deposition, comprising a two-step process and has been widely used in the fabrication of ZnO-based mechanical energy-harvesting devices [126,127].

The schematic flow process of ECD ZnO NRs is depicted in Figure 13. ZnO NRs are grown on top of a ZnO seed layer placed on the conductive substrate (working electrode) as the seed layer to provide a nucleation site for the growth of ZnO NRs [127]. The ZnO seed layer is pre-deposited on an ITO substrate by using RF magnetron sputtering in an inert gas environment. Next, a double junction of Ag/AgCl (reference electrode) and platinum (Pt) foil (counter electrode) is linked to the cathode through an external circuit. Then, both electrodes are immersed in the zinc precursor solution, while magnetic stirring and heating are continuously maintained. The electrochemical process occurs when an external voltage is applied between two electrodes in order to speed up the driving force of the deposition. The electrochemical process begins when the ions mix with ions in the solution, then diffuses to the working electrode, thus resulting in the deposition of ZnO on the ZnO seed layer substrate. Afterward, ZnO NRs are produced by dehydrating $Zn(OH)_2$ units at a temperature between 75 to 80 °C [127].

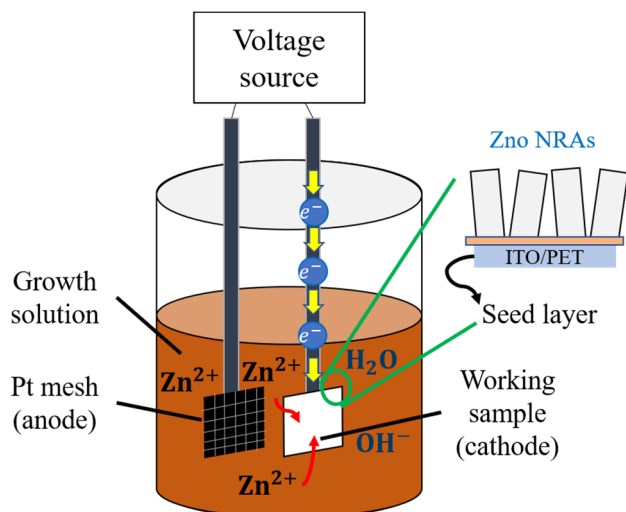


Figure 13. Schematic illustration of ECD.

In this technique, the diameter and length of ZnO NRs can be controlled by the growth time, concentration of the precursor and the external applied voltage. Although the ECD technique has many advantages over other deposition techniques, it is difficult to produce good quality crystals of ZnO NRs due to its low synthesis temperature. Moreover, previous results showed that, with the application of the ECD technique, the ZnO NRs are randomly grown, which causes poor rod termination and poor electrical contact at the counter electrode. Furthermore, the array of ZnO NRs grown on the working electrode has a larger diameter distribution and lower charge carrier density compared to the hydrothermal technique [128]. Therefore, these disadvantages limit its use for PENG fabrication.

6. Recent Technology in Piezoelectric Nanogenerators (PENG)

In recent years, researchers have conceived four methods for improving the performance of ZnO-based PENG output; (i) doping, (ii) increasing the area density of ZnO NRs,

(iii) interface modification and (iv) combination methods. All of these methods have their own characteristics wherein they can compete and complement each other in improving output performance [129].

6.1. Doping

The P-type doping of ZnO NRs is a method to improve the performance of ZnO-based PENGs. It is also a simple approach to increase the piezoelectric output, because p-type doping can reduce the filtering effect in ZnO NRs by replacing the majority of the carriers (electrons) with holes, thus causing the excessive contraction of free electrons. There are several p-type dopants that can be used, such as silver (Ag) [130], lanthanum (La) [131], lithium (Li) [132] and antimony (Sb) [133]. L. Kang et al., investigated the effect of doping on piezoelectric performance using La-doped and undoped ZnO NWs. The study found that, when 5 mol% La-doped ZnO NWs was added, the output voltage increased from 2.1 V to 3.0 V. These results proved that the P-type doping method boosts piezoelectric performance [131]. In addition, the piezoelectric performance of p-type doping has also been proven in [132]. Y. Chang et al. [132] have successfully grown p-type ZnO NWs on Si substrates and claimed that p-type doped ZnO NWs are among the best candidates for nano-generating devices. This is based on an analysis that was carried out on the piezoelectric performance between p-type doped ZnO NWs and pure ZnO NWs through the piezoelectric response. The results show that P-type doped ZnO NWs produce high mobility and effective hole carrier concentration, thus leading to higher piezoelectric output current, power and voltage than pure ZnO NWs.

6.2. Areal Density

As is well known, doping is one of the feasible strategies to overcome the piezoelectric quality of ZnO nanorods. However, the output performance of PENG devices can be further improved by incorporating ZnO NR arrays into complex structures with higher effective NR area density. DM Shin et al., fabricated a two-sided heterostructure of free-standing ZnO NRs/graphene/ZnO NRs. They claim that the double-sided heterostructure produces a coupling of the piezoelectric effect from both the upward and downward growing nanorods, thus resulting in twice the total output voltage and different current density compared to the single heterostructure [119]. M. R. Hassan et al., formed a heterojunction with a Si micropillar (MP) array as the enhancement process in order to enhance the performance of piezoelectric nanogenerators [118]. It is stated that the length of the SiMP array influences the growth and crystalline quality of ZnO NRs and the piezoelectric output voltage. As the length of the SiMP array increases from 0 to 20 mm, the output voltage also increases from 0.7 to 4.0 V. Furthermore, this enhancement process has also been applied to flexible polyester (PS) for both sides [134] and stainless steel (SS) substrates [135]. This improvement process is explained based on the ZnO NRs series connection, which is considered a source of piezoelectric potential.

6.3. Interfacial Modification

Interfacial modifications have been adopted to increase the piezoelectric output power by addressing the main problem of internal and external filtering effects. In this technique, a p–n junction or Schottky contact between ZnO and metal or metal oxide is built, respectively. The interfacial modification technique improves the output performance through two mechanisms. Firstly, the built-in electric field near the p–n junction efficiently consumes the excess electrons in ZnO, thereby reducing the internal screening effect for generated piezoelectric potentials. Secondly, the output performance can be improved through the barrier interface between the Schottky metal and ZnO, as this interfacial modification reduces the carrier concentration and leakage current [136]. Yin et al. [136] formed a (NiO/ZnO) heterojunction at the interface instead of Schottky barrier in order to enhance the piezoelectric performance. The design based on the p–n junction increased the output

voltage to 430 mV, which was 21 times higher while increasing the output current density to 40 nA, which was 13 times higher than the ZnO film nanogenerator.

6.4. Combination Method

The combination method is another method that can be implemented to achieve a good performance of ZnO PENG. The combination method is a method that combines the doping method and the interfacial modification method [63,101]. Liu et al. [63] have combined the doping and the interfacial modification method to synthesize a Cl-doped ZnO/CuO PENGs device. The result of the study, as illustrated in Figure 14, shows that, by using this combination method, the output voltage and current have increased by 2.2 V and 1000 nAcm⁻². This enhancement is caused by the Cl dopant-induced lattice strain along the c-axis of ZnO and the reduction of free electrons at the p-n ZnO/CuO interface. Additionally, tuning the lattice strain along the ZnO c-axis from a compressive to a tensile state can enhance piezoelectric performance. Due to the difference in ionic size between dopants and oxygen elements, this tuning process can be done by substituting halogen dopants from fluorine with other halogen elements like F, I and Br [101].

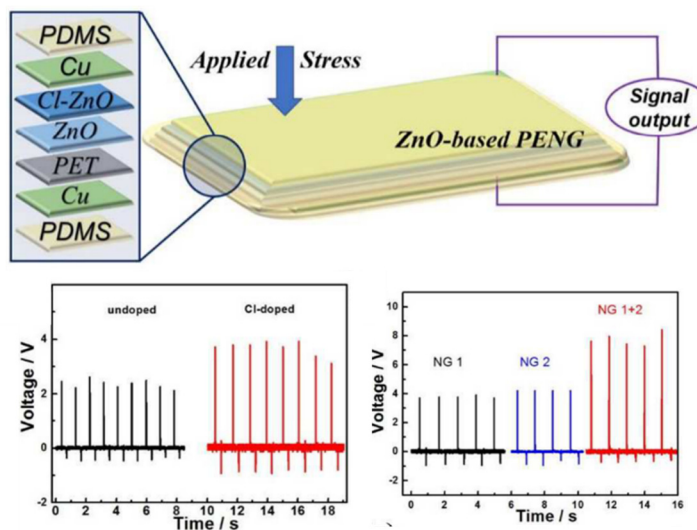


Figure 14. Schematic of Cl-doped ZnO PENGs and its output voltage and the current of the undoped and Cl doped ZnO. Reproduced with permission from reference [63].

7. Discussion

Herein, the progress of PENGs, focusing on piezoelectric semiconductor materials, has been discussed in detail. Based on the description discussed, it has been proven that ZnO NRs have shown good performance compared to other piezoelectric materials. The fact that ZnO NRs can be grown in an orderly and uniform structure. In addition, ZnO NRs have a large surface area allowing the motion to escalate, thus generating more energy. Another piezoelectric material discussed in this paper is lead zirconate titanate (PZT), which has a higher piezoelectric coefficient than other piezoelectric materials, such as barium titanate and ZnO nanorods. However, the PZT nanogenerator is less efficient than the ZnO NGs due to the high piezoelectric coefficient of PZT, causing energy conversion to be less efficient. Furthermore, PZT is not suitable for use at high temperatures, which results in instability and rigidity. The piezoelectric material barium titanate (BaTiO_3) is also promising, with further structural design significantly increasing the piezoelectric response through domain engineering. However, this material has a low piezoelectric coefficient, and no satisfactory application has been found for related piezoelectric devices. Various synthesis techniques have been proposed and applied in producing highly oriented ZnO NRs arrays. The hydrothermal method has proven to be the best route in forming ZnO NRs. It is a simple procedure that requires low temperatures but produces satisfactory results at a reasonable

cost. In addition, it is a rapid and controlled technique that results in a crystal-clear structure with excellent shape and clarity. In short, the alignment of ZnO NRs produced by the hydrothermal technique strongly relies on the crystal orientation of the ZnO seed layer used. A hydrothermal technique was established and can produce ZnO NRs on a large scale in a cost-effective manner. In addition, ZnO NRs have a relatively wide bandgap of 3.3 eV, which is an advantage to ZnO in allowing more energy to be generated. Based on these findings, ZnO possesses exceptional semiconducting and piezoelectric capabilities, relative abundance, low cost, chemical stability in air, bio separation, complexity and several crystal growth techniques. On the other hand, several synthesis techniques have been discussed in this paper. Figure 15 shows the correlation of output power with the aspect ratio based on previously reported synthesis techniques, including hydrothermal, chemical vapor deposition (CVD), thermal evaporation, vapor liquid solid (VLS) and spin coating techniques. The aspect ratio can be controlled by changing the molar concentration of the growth solution and the growth duration. Among the best device performance was obtained through the hydrothermal method, resulting in a high power density output for a piezoelectric nanogenerator. Furthermore, the aspect ratio related to the length and diameter of ZnO NRs is also an important factor in obtaining high performance. Thinner diameters and longer lengths with good alignment tend to bend more easily under external pressure, resulting in efficient piezoelectric generation.

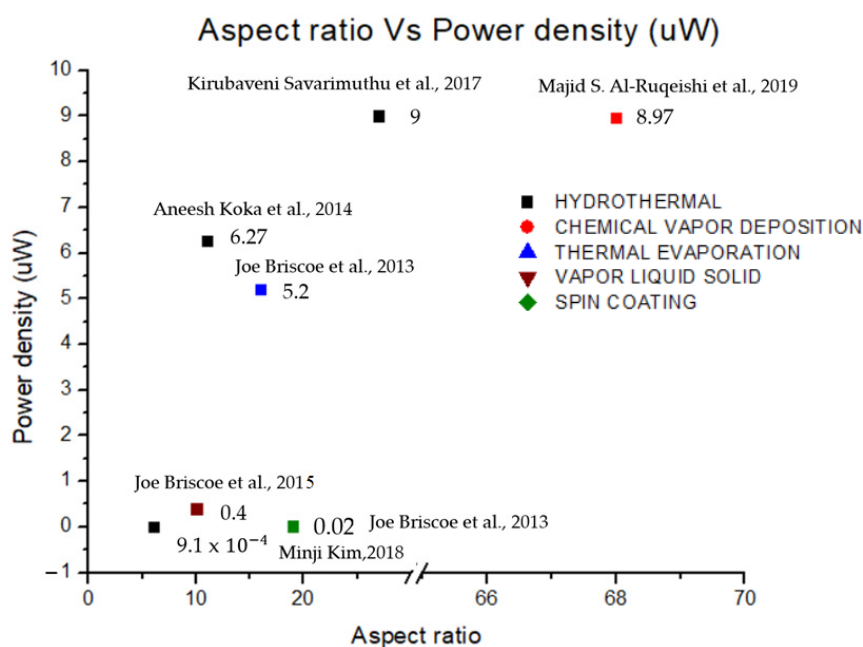


Figure 15. Power density vs. aspect ratio based on several techniques [34,43–45,48,58].

8. Conclusions

The PENGs show high potential in the evolution of the NGs industry. However, continuous studies and modifications are needed to achieve the high performance of PENGs in order to commercialize and compete with other PENGs. Utilizing various micro-morphologies of piezoelectric materials and developing composite thin-film materials are the key strategies for enhancing the performance of piezoelectric nanogenerators. In this paper, several types of piezoelectric materials were discussed, including ZnO NRs, BaTiO₃ and PZT. The ZnO NRs advantages showed good performance due to the wide bandgap semiconductor energy of 3.3 eV, high exciton binding energy (60 meV) and low thermal energy at room temperature (25 meV), which allows stable exciton existence at room temperature. These distinctive properties make ZnO suitable for a number of prospective applications, such as transparent electrodes in optoelectronic and solar cell devices, laser diodes and light-emitting diodes, etc. Apart from that, doping the ZnO NRs also enhanced

performance. Based on this research, Ni-doped ZnO NRs are shown to achieve higher output power compared to other dopings, as well as leading to a higher surface area. The exceptional chemical stability of nickel (Ni) on zinc (Zn) sites qualifies nickel (Ni) as an effective doping element in ZnO for improving its different properties. Besides, several approaches for the synthesis techniques of ZnO nanostructures have been discussed, such as hydrothermal technique, CVD and ECD. In the finding, the hydrothermal technique has attracted considerable interest due to its numerous advantages compared to other techniques. It is a straightforward procedure under a low-temperature condition and results in a high yield at a reasonable cost. In addition, it is a quick and controlled technique that results in a crystal-clear structure with excellent shape and clarity.

Author Contributions: Conceptualization, M.A.M., F.A. and F.A.A.; methodology, M.A.M., F.A., F.A.A., N.S.N., M.S.I.M.Z. and A.N.M.M.; fabricate, M.A.M., F.A. and F.A.A.; validation, M.A.M., F.A., M.M.I. and F.A.A.; investigation, M.A.M., F.A. and F.A.A.; resources, K.S.L. and F.A.; data curation, M.A.M., F.A. and F.A.A.; writing—original draft preparation, M.A.M. and F.A.; writing—review and editing, M.A.M., F.A., F.A.A., N.S.N., M.S.I.M.Z. and A.N.M.M.; visualization, M.M.I.; supervision, F.A. and F.A.A.; project administration, F.A.; funding acquisition, F.A., F.A.A., M.M.I. and A.N.M.M. All authors have read and agreed to the published version of the manuscript.

Funding: This research was funded by Universiti Teknikal Malaysia Melaka, Malaysia under grant PJP/2020/FTKEE/PP/S01748.

Data Availability Statement: Not applicable.

Conflicts of Interest: The authors declare no conflict of interest.

References

1. Noorasid, N.; Arith, F.; Mustafa, A.; Azam, M.; Mahalingam, S.; Chelvanathan, P.; Amin, N. Current advancement of flexible dye sensitized solar cell: A review. *Optik* **2022**, *254*, 168089. [[CrossRef](#)]
2. Owusu, P.A.; Asumadu-Sarkodie, S. A review of renewable energy sources, sustainability issues and climate change mitigation. *Cogent Eng.* **2016**, *3*, 1167990. [[CrossRef](#)]
3. Nguyen, V.; Zhu, R.; Yang, R. Environmental effects on nanogenerators. *Nano Energy* **2015**, *14*, 49–61. [[CrossRef](#)]
4. Lin, Z.; Chen, J.; Yang, J. Recent Progress in Triboelectric Nanogenerators as a Renewable and Sustainable Power Source. *J. Nanomater.* **2016**, *2016*, 5651613. [[CrossRef](#)]
5. Fan, F.-R.; Tian, Z.-Q.; Wang, Z.L. Flexible triboelectric generator. *Nano Energy* **2012**, *1*, 328–334. [[CrossRef](#)]
6. Wang, Z.J.; Wang, D.-J. An RF field pattern with improved B1 amplitude homogeneity. *Concepts Magn. Reson. Part B* **2005**, *24*, 1–5. [[CrossRef](#)]
7. Hu, Y.; Wang, Z.L. Recent progress in piezoelectric nanogenerators as a sustainable power source in self-powered systems and active sensors. *Nano Energy* **2015**, *14*, 3–14. [[CrossRef](#)]
8. Bogue, R. Energy harvesting: A review of recent developments. *Sens. Rev.* **2015**, *35*, 1–5. [[CrossRef](#)]
9. Soin, N. *Magnetic Nanoparticles-Piezoelectric Polymer Nanocomposites for Energy Harvesting*; Elsevier Inc.: Amsterdam, The Netherlands, 2018.
10. Bayramol, D.V.; Soin, N.; Shah, T.; Siories, E.; Matsouka, D.; Vassiliadis, S. *Energy Harvesting Smart Textiles*; Springer: Berlin/Heidelberg, Germany, 2017; pp. 199–231.
11. Harstad, S.; D’Souza, N.; Soin, N.; El-Gendy, A.A.; Gupta, S.; Pecharsky, V.K.; Shah, T.; Siories, E.; Hadimani, R.L. Enhancement of β -phase in PVDF films embedded with ferromagnetic Gd₅Si₄ nanoparticles for piezoelectric energy harvesting. *AIP Adv.* **2017**, *7*, 056411. [[CrossRef](#)]
12. Soin, N.; Shah, T.H.; Anand, S.C.; Geng, J.; Pornwannachai, W.; Mandal, P.; Reid, D.; Sharma, S.; Hadimani, R.L.; Bayramol, D.V.; et al. Novel “3-D spacer” all fibre piezoelectric textiles for energy harvesting applications. *Energy Environ. Sci.* **2014**, *7*, 1670–1679. [[CrossRef](#)]
13. Volk, J.; Nagata, T.; Erdélyi, R.; Bársnyi, I.; Tóth, A.L.; Lukács, I.E.; Czigány, Z.; Tomimoto, H.; Shingaya, Y.; Chikyow, T. Highly Uniform Epitaxial ZnO Nanorod Arrays for Nanopiezotronics. *Nanoscale Res. Lett.* **2009**, *4*, 699–704. [[CrossRef](#)]
14. Dagdeviren, C.; Li, Z.; Wang, Z.L. Energy Harvesting from the Animal/Human Body for Self-Powered Electronics. *Annu. Rev. Biomed. Eng.* **2017**, *19*, 85–108. [[CrossRef](#)]
15. Soin, N.; Anand, S.; Shah, T. *Energy Harvesting and Storage Textiles*, 2nd ed.; Elsevier Ltd.: Amsterdam, The Netherlands, 2016.
16. Bowen, C.R.; Kim, H.A.; Weaver, P.M.; Dunn, S. Piezoelectric and ferroelectric materials and structures for energy harvesting applications. *Energy Environ. Sci.* **2013**, *7*, 25–44. [[CrossRef](#)]
17. Wan, C.; Bowen, C.R. Multiscale-structuring of polyvinylidene fluoride for energy harvesting: The impact of molecular-, micro- and macro-structure. *J. Mater. Chem. A* **2017**, *5*, 3091–3128. [[CrossRef](#)]

18. Ramadan, K.S.; Sameoto, D.; Evoy, S. A review of piezoelectric polymers as functional materials for electromechanical transducers. *Smart Mater. Struct.* **2014**, *23*, 033001. [[CrossRef](#)]
19. Xu, Y.; Yu, Q.; Li, J.-F. A facile method to fabricate vertically aligned $(\text{K},\text{Na})\text{NbO}_3$ lead-free piezoelectric nanorods. *J. Mater. Chem.* **2012**, *22*, 23221–23226. [[CrossRef](#)]
20. Singh, S.; Tripathi, R.K.; Gupta, M.K.; Dzhardimalieva, G.I.; Uflyand, I.E.; Yadav, B. 2-D self-healable polyaniline-polypyrrole nanoflakes based triboelectric nanogenerator for self-powered solar light photo detector with DFT study. *J. Colloid Interface Sci.* **2021**, *600*, 572–585. [[CrossRef](#)]
21. Singh, S.; Yadav, P.; Gupta, M.K.; Dzhardimalieva, G.I.; Yoon, J.; Maiti, C.; Yadav, B.C. Gigantic stimulation in response by solar irradiation in self-healable and self-powered LPG sensor based on triboelectric nanogenerator: Experimental and DFT computational study. *Sens. Actuators B: Chem.* **2022**, *359*, 131573. [[CrossRef](#)]
22. Thakre, A.; Kumar, A.; Song, H.-C.; Jeong, D.-Y.; Ryu, J. Pyroelectric Energy Conversion and Its Applications—Flexible Energy Harvesters and Sensors. *Sensors* **2019**, *19*, 2170. [[CrossRef](#)]
23. Li, X.; Liang, R.; Tao, J.; Peng, Z.; Xu, Q.; Han, X.; Wang, X.; Wang, C.; Zhu, J.; Pan, C.; et al. Flexible Light Emission Diode Arrays Made of Transferred Si Microwires-ZnO Nanofilm with Piezo-Phototronic Effect Enhanced Lighting. *ACS Nano* **2017**, *11*, 3883–3889. [[CrossRef](#)]
24. Li, X.; Chen, M.; Yu, R.; Zhang, T.; Song, D.; Liang, R.; Zhang, Q.; Cheng, S.; Dong, L.; Pan, A.; et al. Enhancing Light Emission of ZnO-Nanofilm/Si-Micropillar Heterostructure Arrays by Piezo-Phototronic Effect. *Adv. Mater.* **2015**, *27*, 4447–4453. [[CrossRef](#)] [[PubMed](#)]
25. Pandey, R.K.; Dutta, J.; Brahma, S.; Rao, B.; Liu, C.-P. Review on ZnO-based piezotronics and piezoelectric nanogenerators: Aspects of piezopotential and screening effect. *J. Phys.: Mater.* **2021**, *4*, 044011. [[CrossRef](#)]
26. Wen, X.; Wu, W.; Pan, C.; Hu, Y.; Yang, Q.; Wang, Z.L. Development and progress in piezotronics. *Nano Energy* **2015**, *14*, 276–295. [[CrossRef](#)]
27. Lu, J.; Xu, C.; Li, F.; Yang, Z.; Peng, Y.; Li, X.; Que, M.; Pan, C.; Wang, Z.L. Piezoelectric Effect Tuning on ZnO Microwire Whispering-Gallery Mode Lasing. *ACS Nano* **2018**, *12*, 11899–11906. [[CrossRef](#)]
28. Jiji, G. A retrospect on the role of piezoelectric nanogenerators in the development of the green world. *RSC Adv.* **2017**, *7*, 33642–33670. [[CrossRef](#)]
29. Song, H. *Fabrication and Characterisation of Electrospun Polyvinylidene Fluoride (PVDF) Nanocomposites for Energy Harvesting Applications*; Brunel University London: London, UK, 2016; p. 147.
30. Ma, J.; Hu, J.; Li, Z.; Nan, C.-W. Recent Progress in Multiferroic Magnetoelectric Composites: From Bulk to Thin Films. *Adv. Mater.* **2011**, *23*, 1062–1087. [[CrossRef](#)]
31. Hu, J.-M.; Li, Z.; Wang, J.; Ma, J.; Lin, Y.H.; Nan, C.W. A simple bilayered magnetoelectric random access memory cell based on electric-field controllable domain structure. *J. Appl. Phys.* **2010**, *108*, 043909. [[CrossRef](#)]
32. Ma, J.; Shi, Z.; Nan, C.-W. Magnetoelectric Properties of Composites of Single $\text{Pb}(\text{Zr},\text{Ti})\text{O}_3$ Rods and Terfenol-D/Epoxy with a Single-Period of 1-3-Type Structure. *Adv. Mater.* **2007**, *19*, 2571–2573. [[CrossRef](#)]
33. Fujii, I.; Nakashima, K.; Kumada, N.; Wada, S. Structural, dielectric, and piezoelectric properties of $\text{BaTiO}_3\text{-Bi}(\text{Ni}_{1/2}\text{Ti}_{1/2})\text{O}_3$ ceramics. *J. Ceram. Soc. Jpn.* **2012**, *120*, 30–34. [[CrossRef](#)]
34. Briscoe, J.; Dunn, S. Piezoelectric nanogenerators—A review of nanostructured piezoelectric energy harvesters. *Nano Energy* **2015**, *14*, 15–29. [[CrossRef](#)]
35. Zhu, G.; Wang, A.C.; Liu, Y.; Zhou, Y.; Wang, Z.L. Functional Electrical Stimulation by Nanogenerator with 58 V Output Voltage. *Nano Lett.* **2012**, *12*, 3086–3090. [[CrossRef](#)] [[PubMed](#)]
36. Qi, Y.; McAlpine, M.C. Nanotechnology-enabled flexible and biocompatible energy harvesting. *Energy Environ. Sci.* **2010**, *3*, 1275–1285. [[CrossRef](#)]
37. Wang, Z.L.; Wu, W. Nanotechnology-Enabled Energy Harvesting for Self-Powered Micro-/Nanosystems. *Angew. Chem. Int. Ed.* **2012**, *51*, 11700–11721. [[CrossRef](#)]
38. Delgado-Alvarado, E.; Elvira-Hern, E.A.; Huerta-Chua, J.; Vázquez-Leal, H.; Mart, J.; Garc, P.J. Recent Progress of Nanogenerators for Green Energy Harvesting: Performance, Applications and Challenges. *Nanomaterials* **2022**, *12*, 2549. [[CrossRef](#)]
39. Wang, Z.L.; Song, J. Piezoelectric Nanogenerators Based on Zinc Oxide Nanowire Arrays. *Science* **2006**, *312*, 242–246. [[CrossRef](#)]
40. Wang, X.; Song, J.; Liu, J.; Wang, Z.L. Direct-Current Nanogenerator Driven by Ultrasonic Waves. *Science* **2007**, *316*, 102–105. [[CrossRef](#)]
41. Hu, D.; Yao, M.; Fan, Y.; Ma, C.; Fan, M.; Liu, M. Strategies to achieve high performance piezoelectric nanogenerators. *Nano Energy* **2019**, *55*, 288–304. [[CrossRef](#)]
42. Bouvet-Marchand, A.; Graillot, A.; Volk, J.; Dauksevicius, R.; Sturm, C.; Grundmann, M.; Saoutieff, E.; Viana, A.; Christian, B.; Lebedev, V.; et al. Design of UV-crosslinked polymeric thin layers for encapsulation of piezoelectric ZnO nanowires for pressure-based fingerprint sensors. *J. Mater. Chem. C* **2017**, *6*, 605–613. [[CrossRef](#)]
43. Al-Ruqeishi, M.; Mohiuddin, T.; Al-Habibi, B.; Al-Ruqeishi, F.; Al-Fahdi, A.; Al-Khusaibi, A. Piezoelectric nanogenerator based on ZnO nanorods. *Arab. J. Chem.* **2019**, *12*, 5173–5179. [[CrossRef](#)]
44. Savarimuthu, K.; Rajamanickam, G.; Shankararajan, R.; Perumal, R.; Rayarfrancis, A. Experimental Study on Flexible ZnO Based Nanogenerator Using Schottky Contact for Energy Harvesting Applications. *IEEE Trans. Nanotechnol.* **2017**, *16*, 469–476. [[CrossRef](#)]

45. Briscoe, J.; Jalali, N.; Wooliams, P.; Stewart, M.; Weaver, P.M.; Cain, M.; Dunn, S. Measurement techniques for piezoelectric nanogenerators. *Energy Environ. Sci.* **2013**, *6*, 3035–3045. [[CrossRef](#)]
46. Cao, P.; Yang, Z.; Navale, S.; Han, S.; Liu, X.; Liu, W.; Lu, Y.; Stadler, F.; Zhu, D. Ethanol sensing behavior of Pd-nanoparticles decorated ZnO-nanorod based chemiresistive gas sensors. *Sens. Actuators B Chem.* **2019**, *298*, 126850. [[CrossRef](#)]
47. Pearton, S.; Norton, D.; Ip, K.; Heo, Y.; Steiner, T. Recent progress in processing and properties of ZnO. *Superlattices Microstruct.* **2003**, *34*, 3–32. [[CrossRef](#)]
48. Koka, A.; Zhou, Z.; Sodano, H.A. Vertically aligned BaTiO₃nanowire arrays for energy harvesting. *Energy Environ. Sci.* **2013**, *7*, 288–296. [[CrossRef](#)]
49. Wu, W.; Bai, S.; Yuan, M.; Qin, Y.; Wang, Z.L.; Jing, T. Lead Zirconate Titanate Nanowire Textile Nanogenerator for Wearable Energy-Harvesting and Self-Powered Devices. *ACS Nano* **2012**, *6*, 6231–6235. [[CrossRef](#)]
50. Ku, N.-J.; Liu, G.; Wang, C.-H.; Gupta, K.; Liao, W.-S.; Ban, D.; Liu, C.-P. Optimal geometrical design of inertial vibration DC piezoelectric nanogenerators based on obliquely aligned InN nanowire arrays. *Nanoscale* **2017**, *9*, 14039–14046. [[CrossRef](#)]
51. Islam, S.; Zamil, Y.; Mojumder, R.H.; Stampfl, C.; Park, J. Strong tribo-piezoelectric effect in bilayer indium nitride (InN). *Sci. Rep.* **2021**, *11*, 18669. [[CrossRef](#)]
52. Mishra, S.; Supraba, P.; Sankar, P.; Kumar, R.; Prakash, K.; Haranath, D. Controlled synthesis of luminescent ZnS nanosheets with high piezoelectric performance for designing mechanical energy harvesting device. *Mater. Chem. Phys.* **2021**, *277*, 125264. [[CrossRef](#)]
53. Parangusan, H.; Bhadra, J.; Al-Thani, N. Flexible piezoelectric nanogenerator based on [P(VDF-HFP)]/PANI-ZnS electrospun nanofibers for electrical energy harvesting. *J. Mater. Sci. Mater. Electron.* **2021**, *32*, 6358–6368. [[CrossRef](#)]
54. Banerjee, S.; Bairagi, S.; Ali, S.W. A lead-free flexible piezoelectric-triboelectric hybrid nanogenerator composed of uniquely designed PVDF/KNN-ZS nanofibrous web. *Energy* **2022**, *244*, 123102. [[CrossRef](#)]
55. Zhao, B.; Chen, Z.; Cheng, Z.; Wang, S.; Yu, T.; Yang, W.; Li, Y. Piezoelectric Nanogenerators Based on Electrospun PVDF-Coated Mats Composed of Multilayer Polymer-Coated BaTiO₃ Nanowires. *ACS Appl. Nano Mater.* **2022**, *5*, 8417–8428. [[CrossRef](#)]
56. He, Y.; Wang, H.; Sha, Z.; Boyer, C.; Wang, C.-H.; Zhang, J. Enhancing output performance of PVDF-HFP fiber-based nanogenerator by hybridizing silver nanowires and perovskite oxide nanocrystals. *Nano Energy* **2022**, *98*, 107343. [[CrossRef](#)]
57. Mallick, Z.; Saini, D.; Sarkar, R.; Kundu, T.K.; Mandal, D. Piezo-phototronic effect in highly stable lead-free double perovskite Cs₂SnI₆-PVDF nanocomposite: Possibility for strain modulated optical sensor. *Nano Energy* **2022**, *100*, 107451. [[CrossRef](#)]
58. Kim, M.; Wu, Y.S.; Kan, E.C.; Fan, J. Breathable and Flexible Piezoelectric ZnO@PVDF Fibrous Nanogenerator for Wearable Applications. *Polymers* **2018**, *10*, 745. [[CrossRef](#)] [[PubMed](#)]
59. Qiu, Y.; Lei, J.; Yang, D.; Yin, B.; Zhang, H.; Bian, J.; Ji, J.; Liu, Y.; Zhao, Y.; Luo, Y.; et al. Enhanced performance of wearable piezoelectric nanogenerator fabricated by two-step hydrothermal process. *Appl. Phys. Lett.* **2014**, *104*, 113903. [[CrossRef](#)]
60. Aleman, C.K.; Narvaez, J.A.B.; Lopez, G.D.B.; Mercado, C.C. Array pattern effects on the voltage output of vertically aligned BaTiO₃ nanotubular flexible piezoelectric nanogenerator. *MRS Commun.* **2020**, *10*, 500–505. [[CrossRef](#)]
61. Khan, A.; Abbasi, M.A.; Hussain, M.; Ibupoto, Z.H.; Wissting, J.; Nur, O.; Willander, M. Piezoelectric nanogenerator based on zinc oxide nanorods grown on textile cotton fabric. *Appl. Phys. Lett.* **2012**, *101*, 193506. [[CrossRef](#)]
62. Chen, X.; Xu, S.; Yao, N.; Xu, W.; Shi, Y. Potential measurement from a single lead zirconate titanate nanofiber using a nanomanipulator. *Appl. Phys. Lett.* **2009**, *94*, 253113. [[CrossRef](#)]
63. Liu, C.; Yu, A.; Peng, M.; Song, M.; Liu, W.; Zhang, Y.; Zhai, J. Improvement in the Piezoelectric Performance of a ZnO Nanogenerator by a Combination of Chemical Doping and Interfacial Modification. *J. Phys. Chem. C* **2016**, *120*, 6971–6977. [[CrossRef](#)]
64. Rafique, S.; Kasi, A.K.; Kasi, J.K.; Aminullah; Bokhari, M.; Shakoor, Z. Fabrication of silver-doped zinc oxide nanorods piezoelectric nanogenerator on cotton fabric to utilize and optimize the charging system. *Nanomater. Nanotechnol.* **2020**, *10*, 1847980419895741. [[CrossRef](#)]
65. Chang, W.-Y.; Fang, T.-H.; Tsai, J.-H. Electromechanical and Photoluminescence Properties of Al-doped ZnO Nanorods Applied in Piezoelectric Nanogenerators. *J. Low Temp. Phys.* **2014**, *178*, 174–187. [[CrossRef](#)]
66. Vayssieres, L.; Keis, K.; Lindquist, S.-E.; Hagfeldt, A. Purpose-Built Anisotropic Metal Oxide Material: 3D Highly Oriented Microrod Array of ZnO. *J. Phys. Chem. B* **2001**, *105*, 3350–3352. [[CrossRef](#)]
67. Fang, T.-H.; Kang, S.-H. Surface and physical characteristics of ZnO:Al nanostructured films. *J. Appl. Phys.* **2009**, *105*, 113512. [[CrossRef](#)]
68. Chu, Y.-L.; Young, S.-J.; Ji, L.-W.; Chu, T.-T.; Chen, P.-H. Synthesis of Ni-Doped ZnO Nanorod Arrays by Chemical Bath Deposition and Their Application to Nanogenerators. *Energies* **2020**, *13*, 2731. [[CrossRef](#)]
69. Parangusan, H.; Ponnamma, D.; AlMaadeed, M.A.A. Flexible tri-layer piezoelectric nanogenerator based on PVDF-HFP/Ni-doped ZnO nanocomposites. *RSC Adv.* **2017**, *7*, 50156–50165. [[CrossRef](#)]
70. Batra, K.; Sinha, N.; Goel, S.; Yadav, H.; Joseph, A.J.; Kumar, B. Enhanced dielectric, ferroelectric and piezoelectric performance of Nd-ZnO nanorods and their application in flexible piezoelectric nanogenerator. *J. Alloy. Compd.* **2018**, *767*, 1003–1011. [[CrossRef](#)]
71. Pandey, R.; Khandelwal, G.; Palani, I.A.; Singh, V.; Kim, S.-J. A La-doped ZnO ultra-flexible flutter-piezoelectric nanogenerator for energy harvesting and sensing applications: A novel renewable source of energy. *Nanoscale* **2019**, *11*, 14032–14041. [[CrossRef](#)]
72. Batra, K.; Sinha, N.; Kumar, B. Tb-doped ZnO:PDMS based flexible nanogenerator with enhanced piezoelectric output performance by optimizing nanofiller concentration. *Ceram. Int.* **2020**, *46*, 24120–24128. [[CrossRef](#)]

73. Sinha, N.; Ray, G.; Bhandari, S.; Godara, S.; Kumar, B. Synthesis and enhanced properties of cerium doped ZnO nanorods. *Ceram. Int.* **2014**, *40*, 12337–12342. [\[CrossRef\]](#)
74. Gupta, M.K.; Lee, J.-H.; Lee, K.Y.; Kim, S.-W. Two-Dimensional Vanadium-Doped ZnO Nanosheet-Based Flexible Direct Current Nanogenerator. *ACS Nano* **2013**, *7*, 8932–8939. [\[CrossRef\]](#)
75. Batra, K.; Sinha, N.; Kumar, B. Ba-doped ZnO nanorods: Efficient piezoelectric filler material for PDMS based flexible nanogenerator. *Vacuum* **2021**, *191*, 110385. [\[CrossRef\]](#)
76. Lee, J.-H.; Lee, K.Y.; Kumar, B.; Kim, S.-W. Synthesis of Ga-Doped ZnO Nanorods Using an Aqueous Solution Method for a Piezoelectric Nanogenerator. *J. Nanosci. Nanotechnol.* **2012**, *12*, 3430–3433. [\[CrossRef\]](#)
77. Sinha, N.; Ray, G.; Godara, S.; Gupta, M.K.; Kumar, B. Enhanced piezoelectric output voltage and Ohmic behavior in Cr-doped ZnO nanorods. *Mater. Res. Bull.* **2014**, *59*, 267–271. [\[CrossRef\]](#)
78. Lam, K.-T.; Chu, Y.-L.; Ji, L.-W.; Hsiao, Y.-J.; Chu, T.-T.; Huang, B.-W. Characterization of nanogenerators based on S-doped zinc oxide nanorod arrays. *Microsyst. Technol.* **2020**, *28*, 395–401. [\[CrossRef\]](#)
79. Ng, Z.-N.; Chan, K.-Y.; Tohsophon, T. Effects of annealing temperature on ZnO and AZO films prepared by sol-gel technique. *Appl. Surf. Sci.* **2012**, *258*, 9604–9609. [\[CrossRef\]](#)
80. Jain, S.; Karmakar, N.; Shah, A.; Shimpi, N.G. Development of Ni doped ZnO/polyaniline nanocomposites as high response room temperature NO₂ sensor. *Mater. Sci. Eng. B* **2019**, *247*, 114381. [\[CrossRef\]](#)
81. Fang, T.-H. Physical Properties of ZnO: Al Nanorods for Piezoelectric Nanogenerator Application. *Curr. Nanosci.* **2010**, *6*, 505–511. [\[CrossRef\]](#)
82. Rajabi, M.; Ghorbani, M. Performance evaluation of nanogenerators based on Ag doped ZnO nanorods. *Sens. Actuators A Phys.* **2017**, *266*, 338–344. [\[CrossRef\]](#)
83. Hasanpoor, M.; Aliofkhaizraei, M.; Delavari, H. In-situ study of mass and current density for electrophoretic deposition of zinc oxide nanoparticles. *Ceram. Int.* **2016**, *42*, 6906–6913. [\[CrossRef\]](#)
84. Kołodziejczak-Radzimska, A.; Jesionowski, T. Zinc Oxide—From Synthesis to Application: A Review. *Materials* **2014**, *7*, 2833–2881. [\[CrossRef\]](#)
85. Qin, C.; Gu, Y.; Sun, X.; Wang, X.; Zhang, Y. Structural dependence of piezoelectric size effects and macroscopic polarization in ZnO nanowires: A first-principles study. *Nano Res.* **2015**, *8*, 2073–2081. [\[CrossRef\]](#)
86. Cauda, V.; Stassi, S.; Lamberti, A.; Morello, M.; Pirri, C.F.; Canavese, G. Leveraging ZnO morphologies in piezoelectric composites for mechanical energy harvesting. *Nano Energy* **2015**, *18*, 212–221. [\[CrossRef\]](#)
87. Tlemcani, T.S.; Justeau, C.; Nadaud, K.; Poulin-Vitrant, G.; Alquier, D. Deposition Time and Annealing Effects of ZnO Seed Layer on Enhancing Vertical Alignment of Piezoelectric ZnO Nanowires. *Chemosensors* **2019**, *7*, 7. [\[CrossRef\]](#)
88. Joshi, S.; Nayak, M.; Rajanna, K. Effect of post-deposition annealing on transverse piezoelectric coefficient and vibration sensing performance of ZnO thin films. *Appl. Surf. Sci.* **2014**, *296*, 169–176. [\[CrossRef\]](#)
89. Sohn, J.I.; Cha, S.N.; Song, B.G.; Lee, S.; Kim, S.M.; Ku, J.; Kim, H.J.; Park, Y.J.; Choi, B.L.; Wang, Z.L.; et al. Engineering of efficiency limiting free carriers and an interfacial energy barrier for an enhancing piezoelectric generation. *Energy Environ. Sci.* **2012**, *6*, 97–104. [\[CrossRef\]](#)
90. Pham, T.T.; Lee, K.Y.; Lee, J.; Kim, K.H.; Shin, K.S.; Gupta, M.K.; Kumar, B.; Kim, S. Reliable operation of a nanogenerator under ultraviolet light via engineering piezoelectric potential. *Energy Environ. Sci.* **2013**, *6*, 841–846. [\[CrossRef\]](#)
91. Cha, S.N.; Seo, J.-S.; Kim, S.M.; Kim, H.J.; Park, Y.J.; Kim, S.-W.; Kim, J.M. Sound-Driven Piezoelectric Nanowire-Based Nanogenerators. *Adv. Mater.* **2010**, *22*, 4726–4730. [\[CrossRef\]](#)
92. Barreca, D.; Bekermann, D.; Comini, E.; Devi, A.; Fischer, R.A.; Gasparotto, A.; Maccato, C.; Sberveglieri, G.; Tondello, E. 1D ZnO nano-assemblies by Plasma-CVD as chemical sensors for flammable and toxic gases. *Sens. Actuators B Chem.* **2010**, *149*, 1–7. [\[CrossRef\]](#)
93. Phan, T.-L.; Yu, S.; Vincent, R.; Dan, N.; Shi, W. Photoluminescence properties of various CVD-grown ZnO nanostructures. *J. Lumin.* **2010**, *130*, 1142–1146. [\[CrossRef\]](#)
94. Lee, D.J.; Park, J.Y.; Yun, Y.S.; Hong, Y.S.; Moon, J.H.; Lee, B.-T.; Kim, S.S. Comparative studies on the growth behavior of ZnO nanorods by metalorganic chemical vapor deposition depending on the type of substrates. *J. Cryst. Growth* **2004**, *276*, 458–464. [\[CrossRef\]](#)
95. Kumar, B.; Lee, K.Y.; Park, H.; Chae, S.J.; Lee, Y.H.; Kim, S. Controlled Growth of Semiconducting Nanowire, Nanowall, and Hybrid Nanostructures on Graphene for Piezoelectric Nanogenerators. *Acs Nano* **2011**, *5*, 4197–4204. [\[CrossRef\]](#) [\[PubMed\]](#)
96. Zhang, D.; Wang, C.; Zhang, F. Oxygen pressure and measurement temperature dependence of defects related bands in zinc oxide films. *Vacuum* **2010**, *85*, 160–163. [\[CrossRef\]](#)
97. Menzel, A.; Subannajui, K.; Bakhda, R.; Wang, Y.; Thomann, R.; Zacharias, M. Tuning the Growth Mechanism of ZnO Nanowires by Controlled Carrier and Reaction Gas Modulation in Thermal CVD. *J. Phys. Chem. Lett.* **2012**, *3*, 2815–2821. [\[CrossRef\]](#)
98. Ghosh, M.; Rao, M.G. Growth mechanism of ZnO nanostructures for ultra-high piezoelectric d33 coefficient. *Mater. Express* **2013**, *3*, 319–327. [\[CrossRef\]](#)
99. Vayssières, L. Growth of Arrayed Nanorods and Nanowires of ZnO from Aqueous Solutions. *Adv. Mater.* **2003**, *15*, 464–466. [\[CrossRef\]](#)

100. Poulin-Vittrant, G.; Oshman, C.; Opoku, C.; Dahiya, A.; Camara, N.; Alquier, D.; Hue, L.-P.T.H.; Lethiecq, M. Fabrication and Characterization of ZnO Nanowire-based Piezoelectric Nanogenerators for Low Frequency Mechanical Energy Harvesting. *Phys. Procedia* **2015**, *70*, 909–913. [CrossRef]
101. Zhang, Y.; Liu, C.; Liu, J.; Xiong, J.; Liu, J.; Zhang, K.; Liu, Y.; Peng, M.; Yu, A.; Zhang, A.; et al. Lattice Strain Induced Remarkable Enhancement in Piezoelectric Performance of ZnO-Based Flexible Nanogenerators. *ACS Appl. Mater. Interfaces* **2016**, *8*, 1381–1387. [CrossRef]
102. Stassi, S.; Cauda, V.; Ottone, C.; Chiodoni, A.; Pirri, C.F.; Canavese, G. Flexible piezoelectric energy nanogenerator based on ZnO nanotubes hosted in a polycarbonate membrane. *Nano Energy* **2015**, *13*, 474–481. [CrossRef]
103. Nour, E.; Sandberg, M.; Willander, M.; Nur, O. Handwriting enabled harvested piezoelectric power using ZnO nanowires/polymer composite on paper substrate. *Nano Energy* **2014**, *9*, 221–228. [CrossRef]
104. Liao, Q.; Zhang, Z.; Zhang, X.; Mohr, M.; Zhang, Y.; Fecht, H.-J. Flexible piezoelectric nanogenerators based on a fiber/ZnO nanowires/paper hybrid structure for energy harvesting. *Nano Res.* **2014**, *7*, 917–928. [CrossRef]
105. Saravananakumar, B.; Kim, S.-J. Growth of 2D ZnO Nanowall for Energy Harvesting Application. *J. Phys. Chem. C* **2014**, *118*, 8831–8836. [CrossRef]
106. Zhang, Z.; Chen, Y.; Guo, J. ZnO nanorods patterned-textile using a novel hydrothermal method for sandwich structured-piezoelectric nanogenerator for human energy harvesting. *Phys. E: Low-Dimens. Syst. Nanostructures* **2018**, *105*, 212–218. [CrossRef]
107. Khan, A.; Hussain, M.; Nur, O.; Willander, M. Mechanical and piezoelectric properties of zinc oxide nanorods grown on conductive textile fabric as an alternative substrate. *J. Phys. D Appl. Phys.* **2014**, *47*, 345102. [CrossRef]
108. Khan, A.; Hussain, M.; Nur, O.; Willander, M. Fabrication of zinc oxide nanoneedles on conductive textile for harvesting piezoelectric potential. *Chem. Phys. Lett.* **2014**, *612*, 62–67. [CrossRef]
109. Zang, W.; Wang, W.; Zhu, D.; Xing, L.; Xue, X. Humidity-dependent piezoelectric output of Al-ZnO nanowire nanogenerator and its applications as a self-powered active humidity sensor. *RSC Adv.* **2014**, *4*, 56211–56215. [CrossRef]
110. Hussain, M.; Abbasi, M.A.; Ibupoto, Z.H.; Nur, O.; Willander, M. The improved piezoelectric properties of ZnO nanorods with oxygen plasma treatment on the single layer graphene coated polymer substrate. *Phys. Status Solidi* **2014**, *211*, 455–459. [CrossRef]
111. Opoku, C.; Dahiya, A.S.; Oshman, C.; Cayrel, F.; Poulin-Vittrant, G.; Alquier, D.; Camara, N. Fabrication of ZnO Nanowire Based Piezoelectric Generators and Related Structures. *Phys. Procedia* **2015**, *70*, 858–862. [CrossRef]
112. Lee, C.-T.; Chiu, Y.-S. Piezoelectric ZnO-nanorod-structured pressure sensors using GaN-based field-effect-transistor. *Appl. Phys. Lett.* **2015**, *106*, 073502. [CrossRef]
113. Lei, J.; Yin, B.; Qiu, Y.; Zhang, H.; Chang, Y.; Luo, Y.; Zhao, Y.; Ji, J.; Hu, L. Flexible piezoelectric nanogenerator based on Cu₂O-ZnO p-n junction for energy harvesting. *RSC Adv.* **2015**, *5*, 59458–59462. [CrossRef]
114. Wang, Q.; Yang, D.; Qiu, Y.; Zhang, X.; Song, W.; Hu, L. Two-dimensional ZnO nanosheets grown on flexible ITO-PET substrate for self-powered energy-harvesting nanodevices. *Appl. Phys. Lett.* **2018**, *112*, 063906. [CrossRef]
115. Zhang, X.; Yang, D.; Qiu, Y.; Nie, Y.; Chu, H.; Zhang, H.; Hu, L. Improvement in the Piezoelectric Performance of a ZnO Nanogenerator by a ZnO/Spiro-MeOTAD ps-n Heterojunction. *Phys. Status Solidi* **2019**, *216*, 1800717. [CrossRef]
116. Lu, S.; Liao, Q.; Qi, J.; Liu, S.; Liu, Y.; Liang, Q.; Zhang, G.; Zhang, Y. The enhanced performance of piezoelectric nanogenerator via suppressing screening effect with Au particles/ZnO nanoarrays Schottky junction. *Nano Res.* **2015**, *9*, 372–379. [CrossRef]
117. Pan, C.; Chen, Y.; Hsieh, C.; Lin, C.-H.; Su, C.; Yen, C.; Liu, Z.; Wang, W. Ultrasonic sensing device with ZnO piezoelectric nanorods by selectively electrospraying method. *Sens. Actuators A: Phys.* **2014**, *216*, 318–327. [CrossRef]
118. Hasan, R.; Baek, S.-H.; Seong, K.S.; Kim, J.H.; Park, I.-K. Hierarchical ZnO Nanorods on Si Micropillar Arrays for Performance Enhancement of Piezoelectric Nanogenerators. *ACS Appl. Mater. Interfaces* **2015**, *7*, 5768–5774. [CrossRef]
119. Shin, D.-M.; Tsege, E.L.; Kang, S.H.; Seung, W.; Kim, S.-W.; Kim, H.K.; Hong, S.W.; Hwang, Y.-H. Freestanding ZnO nanorod/graphene/ZnO nanorod epitaxial double heterostructure for improved piezoelectric nanogenerators. *Nano Energy* **2015**, *12*, 268–277. [CrossRef]
120. Shin, C.; Heo, J.; Park, J.; Lee, T.; Ryu, H.; Shin, B.; Lee, W.; Kim, H.-K. The effect of pH on ZnO hydrothermal growth on PES flexible substrates. *Phys. E: Low-Dimens. Syst. Nanostructures* **2010**, *43*, 54–57. [CrossRef]
121. Tao, Y.; Fu, M.; Zhao, A.; He, D.; Wang, Y. The effect of seed layer on morphology of ZnO nanorod arrays grown by hydrothermal method. *J. Alloy. Compd.* **2010**, *489*, 99–102. [CrossRef]
122. Tak, Y.; Yong, K. Controlled Growth of Well-Aligned ZnO Nanorod Array Using a Novel Solution Method. *J. Phys. Chem. B* **2005**, *109*, 19263–19269. [CrossRef]
123. Kim, H.; Kim, E.; Kim, S. Growth of ZnO Nanorods on ITO Film for Piezoelectric Nanogenerators. *Materials* **2021**, *14*, 1461. [CrossRef]
124. Kruckiewicz, K.; Zak, J.K. Electrochemistry role in production of nano-coatings. In *Comprehensive Guide for Nanocoatings Technology*; Nova Science Publishers: Hauppauge, NY, USA, 2015; pp. 1–33.
125. Kumar, M.; Sasikumar, C. Electrodeposition of Nanostructured ZnO Thin Film: A Review. *Am. J. Mater. Sci. Eng.* **2014**, *2*, 18–23. [CrossRef]
126. Tamvakos, D.; Lepadatu, S.; Antohe, V.-A.; Tamvakos, A.; Weaver, P.M.; Piraux, L.; Cain, M.G.; Pullini, D. Piezoelectric properties of template-free electrochemically grown ZnO nanorod arrays. *Appl. Surf. Sci.* **2015**, *356*, 1214–1220. [CrossRef]

127. Nagaraju, G.; Ko, Y.H.; Yu, J.S. Effect of diameter and height of electrochemically-deposited ZnO nanorod arrays on the performance of piezoelectric nanogenerators. *Mater. Chem. Phys.* **2015**, *149–150*, 393–399. [[CrossRef](#)]
128. Leprince-Wang, Y. *Piezoelectric ZnO Nanostructure for Energy Harvesting*; John Wiley & Sons: Hoboken, NJ, USA, 2015; Volume 1, pp. 1–124. [[CrossRef](#)]
129. Le, A.T.; Ahmadipour, M.; Pung, S.-Y. A review on ZnO-based piezoelectric nanogenerators: Synthesis, characterization techniques, performance enhancement and applications. *J. Alloy. Compd.* **2020**, *844*, 156172. [[CrossRef](#)]
130. Lee, S.; Lee, J.; Ko, W.; Cha, S.; Sohn, J.; Kim, J.; Park, J.; Park, Y.; Hong, J. Solution-processed Ag-doped ZnO Nanowires grown on Flexible Polyester for Wearable Nanogenerator Applications. *Nanoscale* **2013**, *5*, 207890. [[CrossRef](#)]
131. Kang, L.; An, H.; Park, J.Y.; Hong, M.H.; Nahm, S.; Lee, C.G. La-doped p-type ZnO nanowire with enhanced piezoelectric performance for flexible nanogenerators. *Appl. Surf. Sci.* **2019**, *475*, 969–973. [[CrossRef](#)]
132. Chang, Y.-T.; Chen, J.-Y.; Yang, T.-P.; Huang, C.-W.; Chiu, C.-H.; Yeh, P.-H.; Wu, W.-W. Excellent piezoelectric and electrical properties of lithium-doped ZnO nanowires for nanogenerator applications. *Nano Energy* **2014**, *8*, 291–296. [[CrossRef](#)]
133. Laurenti, M.; Canavese, G.; Sacco, A.; Fontana, M.; Bejtka, K.; Castellino, M.; Pirri, C.F.; Cauda, V. Nanobranched ZnO Structure: P-Type Doping Induces Piezoelectric Voltage Generation and Ferroelectric-Photovoltaic Effect. *Adv. Mater.* **2015**, *27*, 4218–4223. [[CrossRef](#)]
134. Hu, Y.; Lin, L.; Zhang, Y.; Wang, Z.L. Replacing a Battery by a Nanogenerator with 20 V Output. *Adv. Mater.* **2011**, *24*, 110–114. [[CrossRef](#)]
135. Jung, D.-Y.; Baek, S.-H.; Hasan, R.; Park, I.-K. Performance-enhanced ZnO nanorod-based piezoelectric nanogenerators on double-sided stainless steel foil. *J. Alloy. Compd.* **2015**, *641*, 163–169. [[CrossRef](#)]
136. Yin, B.; Qiu, Y.; Zhang, H.; Lei, J.; Chang, Y.; Ji, J.; Luo, Y.; Zhao, Y.; Hu, L. Piezoelectric performance enhancement of ZnO flexible nanogenerator by a NiO–ZnO p–n junction formation. *Nano Energy* **2015**, *14*, 95–101. [[CrossRef](#)]